Research Paper

Suppression of p16 alleviates the senescence-associated secretory phenotype

Raquel Buj[1], Kelly E. Leon[1,2], Marlyn A. Anguelov[1], Katherine M. Aird[1]

[1]Department of Pharmacology and Chemical Biology, UPMC Hillman Cancer Center, University of Pittsburgh School of Medicine, Pittsburgh, PA 15213, USA
[2]Biomedical Sciences Graduate Program, Penn State College of Medicine, Hershey, PA 17033, USA

Correspondence to: Raquel Buj, Katherine M. Aird; **email:** bujgomezr@upmc.edu, kaa140@pitt.edu
Keywords: interleukin-6, interleukin-8, LMNB1, inflammation, melanoma
Received: August 20, 2020 **Accepted:** January 21, 2021 **Published:** February 6, 2021

ABSTRACT

Oncogene-induced senescence (OIS) is characterized by increased expression of the cell cycle inhibitor p16, leading to a hallmark cell cycle arrest. Suppression of p16 in this context drives proliferation, senescence bypass, and contributes to tumorigenesis. OIS cells are also characterized by the expression and secretion of a widely variable group of factors collectively termed the senescence-associated secretory phenotype (SASP). The SASP can be both beneficial and detrimental and affects the microenvironment in a highly context-dependent manner. The relationship between p16 suppression and the SASP remains unclear. Here, we show that knockdown of p16 decreases expression of the SASP factors and pro-inflammatory cytokines *IL6* and *CXCL8* in multiple models, including OIS and DNA damage-induced senescence. Notably, this is uncoupled from the senescence-associated cell cycle arrest. Moreover, low p16 expression in both cancer cell lines and patient samples correspond to decreased SASP gene expression, suggesting this is a universal effect of loss of p16 expression. Together, our data suggest that p16 regulates SASP gene expression, which has implications for understanding how p16 modulates both the senescent and tumor microenvironment.

INTRODUCTION

Senescence is considered a state of stable cell cycle arrest that can occur due to a variety of stimuli [1]. Oncogene-induced senescence (OIS) occurs upon activation of an oncogene such as HRAS or BRAF in normal cells [2, 3]. One of the hallmarks of senescent cells is upregulation of the cell cycle inhibitor *CDKN2A* (encoding for p16), which restrains cell cycle progression and cellular proliferation [4–6]. Canonically, elevated p16 represses hyperphosphorylation of the retinoblastoma protein (RB), which inhibits E2F transcription factor-mediated expression of proliferative genes [7]. Loss of p16 is a common event in human cancer that has been linked to senescence bypass, increased proliferation, and malignant transformation though both canonical and non-canonical (RB-independent) pathways [8–12].

The acquisition of a senescence-associated secretory phenotype (SASP) is also characteristic of senescent cells [13]. The SASP is composed of a variety of soluble signaling factors including pro-inflammatory cytokines, chemokines, and growth factors, as well as proteases, insoluble extracellular matrix proteins and non-protein components that are transcriptionally and translationally upregulated and secreted into the surrounding microenvironment by senescent cells [14–18]. Due to the impact that SASP can exert on cellular physiology, this program is tightly regulated at multiple levels. At the transcriptional level, several transcription factors (NF-κB, C/EBP-β) and upstream regulators (p38 MAPK, GATA4, p53, and ATM) have been described to either positively or negatively regulate SASP gene expression [16, 19–25]. The SASP is also regulated at both the epigenetic [26–32] and translational level [17, 33]. Recent publications suggest that the initiation of

SASP gene transcription during OIS is likely due to loss of lamin B1 (*LMNB1*) and nuclear integrity [34, 35], leading to the accumulation of cytoplasmic chromatin fragments (CCFs) [36, 37]. CCFs activate the cytosolic DNA sensor cyclic guanosine monophosphate (GMP)-adenosine monophosphate (AMP) synthase (cGAS) that catalyzes the synthesis of the second messenger cyclic GMP-AMP (cGAMP) to bind and activate stimulator of interferon genes (STING), leading to NF-κB activation and cytokine transcription [36, 38, 39]. Therefore, changes in *LMNB1* expression are tightly linked to SASP gene transcription.

It is well documented that the SASP modifies the cellular microenvironment and alters neighboring cells, exerting a pleiotropic effect that is not fully understood [40]. On one hand, SASP factors contribute to wound-healing [41–43], normal development [44, 45], and have tumor suppressive effects through the recruitment of different immune cells to clear premalignant cells, a process termed senescence surveillance [46–48]. On the other hand, SASP factors can be pro-tumorigenic by sustaining proliferation, invasion, metastasis, and chemoresistance [49–53]. This paradoxical double role of SASP factors is highly dependent on both genetic background and SASP composition, which is known to be both variable and dynamic [54]. Different genetic backgrounds, cellular contexts, and/or senescence inducers allow for different SASP programs that can promote or inhibit tumorigenesis [55–57]. Interestingly, different SASP programs can also induce senescence in neighboring cells in a paracrine manner that in turn express a particular SASP program [55]. Thus, the final beneficial or detrimental net effect of the SASP is governed by multiple mechanisms that are not yet fully understood [58]. Characterizing whether different genetic backgrounds lead to different SASP programs may be critical to develop efficient and personalized regimens for cancer patients. As ~50% of all human tumors have low p16 expression [59], understanding its role in regulating the SASP has implications for a large subset of patients.

Here, we investigated the effect of p16 suppression on SASP gene expression. We found that knockdown of p16 leads to decreased *IL6* and *CXCL8* (encoding IL8) SASP gene expression in both $HRAS^{G12V}$ and $BRAF^{V600E}$ models of OIS. This was not due to increased *LMNB1* expression or loss of senescence markers, indicating that these changes were not due to inhibition of upstream signaling or a simple artifact due to reduced senescence. We confirmed these results in p16-wildtype melanoma cells upon knockdown of p16 and in DNA damage-induced senescence. Moreover, using publicly-available data, we found that low *CDKN2A* expression in patient tumors is associated with a decrease in specific SASP programs. Together, our results suggest that p16 may have a role in transcriptionally regulating SASP factors, which has implications for understanding how loss of p16 affects the senescent and tumor microenvironment.

RESULTS

Knockdown of p16 abrogates oncogene-induced *IL6* and *CXCL8* expression

Upregulation of both p16 and SASP factors are characteristic of OIS cells [13]. A previous study found that overexpression of p16 induces senescence without upregulation of the SASP [60]. However, it is unknown whether p16 upregulation is necessary for SASP gene expression in the context of OIS. In order to better understand the effects of p16 expression on the SASP, we assessed the expression of the most extensively characterized interleukins upregulated in senescence, IL6 and CXCL8 [13, 16, 61]. Knockdown of p16 with $BRAF^{V600E}$ or $HRAS^{G12V}$ overexpression (Supplementary Figure 1A) decreased *IL6* and *CXCL8* expression and suppressed senescence-associated β-galactosidase (SA-β-gal) activity and the cell cycle arrest in IMR90 fibroblasts (Figure 1A–1J), a classical model of OIS [5, 62]. Note that abrogation of p16 expression using these conditions occurs prior to the induction of senescence that typically occurs 2-3 days after oncogene activation [5, 63–65]. A second shRNA targeting p16 confirmed the results, suggesting these observations are not due to off-target effects (Supplementary Figure 1B–1F). Similar results were observed in normal skin fibroblasts Hs 895.Sk (Supplementary Figure 1G, 1H), suggesting this is not a cell line-specific phenomenon. Additionally, knockdown of p16 in the $BRAF^{V600E}$-induced senescence model decreased the expression of other SASP factors including growth factors, proteases, and ligands (Supplementary Figure 1I), suggesting that this is a broader phenomenon not limited to *IL6* and *CXCL8*. Together, these data suggest that knockdown of p16 may regulate the expression of multiple SASP factors upon oncogene activation.

Knockdown of p16 prior to the induction of $BRAF^{V600E}$/$HRAS^{G12V}$-mediated senescence bypasses the senescence-associated cell cycle arrest (Figure 1A–1H and Supplementary Figure 1B–1E) [8]. Therefore, it is possible that the SASP expression is low because the cells never undergo OIS. To investigate whether the observed decrease in *IL6* and *CXCL8* is a direct effect of p16 suppression and not simply a consequence of senescence bypass, we knocked down p16 at two time points after oncogene expression (Figure 2A and Supplementary Figure 2A–2C). Suppression of p16 at day 8 and 10 after oncogene expression did not

bypass senescence as observed using multiple markers of senescence (Figure 2B–2D and Supplementary Figure 2D–2G). Consistent with observations using knockdown of p16 prior to senescence induction (Figure 1), *IL6* and *CXCL8* expression were both decreased when p16 was knocked down at later time points (Figure 2E and Supplementary Figure 2H). All together, these data suggest that the observed effects of p16 expression on *IL6* and *CXCL8* are uncoupled from senescence bypass.

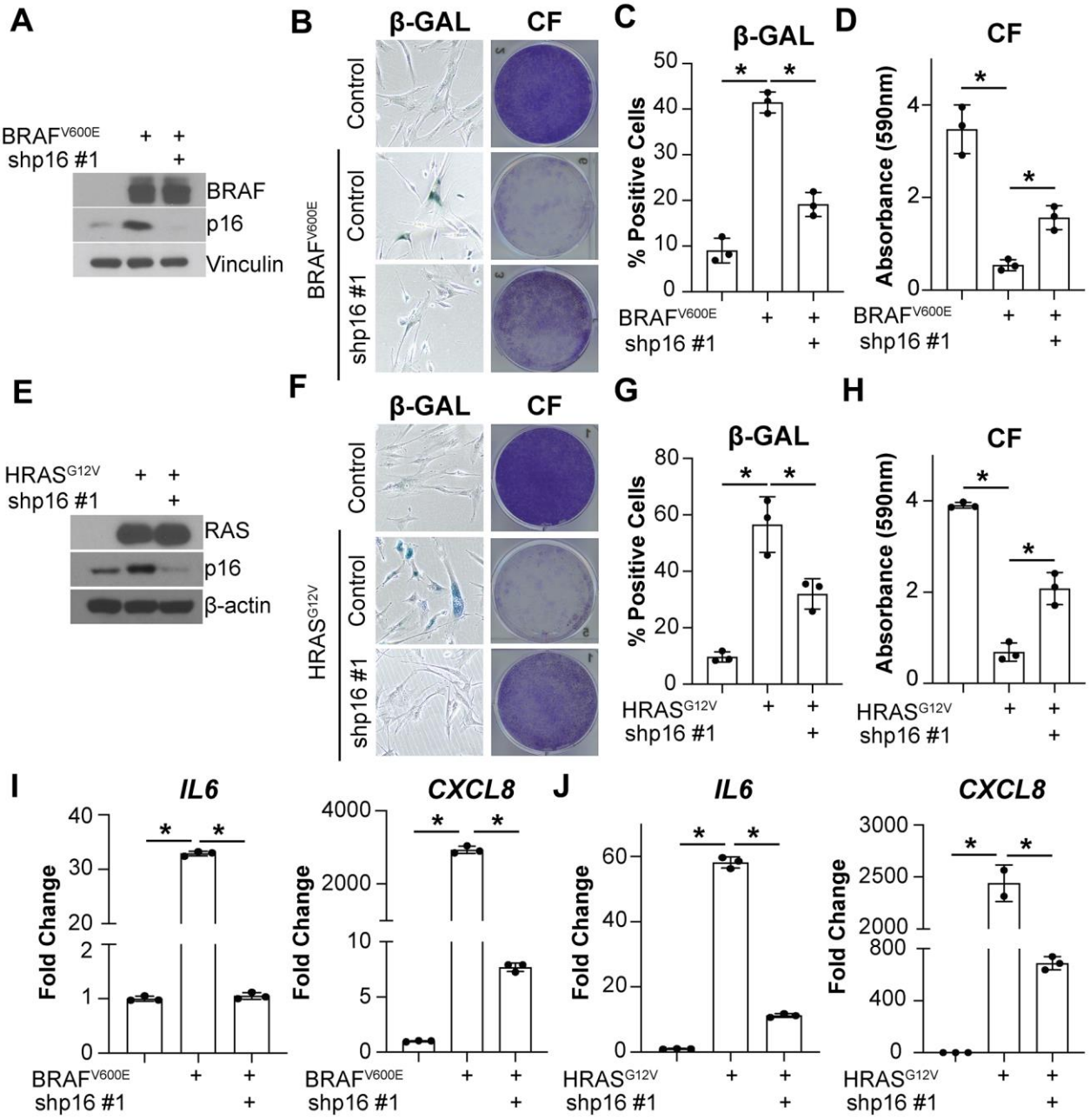

Figure 1. Knockdown of p16 decreases *IL6* and *CXCL8* expression in oncogene-induced senescent cells. IMR90s expressing either BRAF^{V600E} or HRAS^{G12V} alone or in combination with a shRNA targeting p16 (shp16 hairpin #1). An empty pBabe retroviral vector and a shRNA targeting GFP lentiviral vector were used as controls. See Supplementary Figure 1A for an experimental timeline. (**A**) Immunoblot of BRAF and p16. Vinculin was used a loading control. (**B**) Representative images of senescence-associated β-galactosidase (β-GAL) staining and colony formation (CF). (**C**) Quantification of β-GAL in (**B**). (**D**) Quantification of CF in (**B**). (**E**) Immunoblot of RAS and p16. β-actin was used as loading control. (**F**) Representative images of β-GAL staining and colony formation (CF). (**G**) Quantification of β-GAL in (**F**). (**H**) Quantification of CF in (**F**). (**I**, **J**) *IL6* and *CXCL8* mRNA expression (fold change relative to control mean). Expression of target genes was normalized against multiple reference genes. Data normalized against *MRPL9* are shown. n=3/group and mean±SD. 1 out of 3 experiments is shown. *p<0.05.

Knockdown of p16 in tumor cells decreases *IL6* and *CXCL8* expression

Next, we aimed to investigate whether suppression of p16 leads to decreased expression of *IL6* and *CXCL8* in tumor cells. Towards this goal, we knocked down p16 in three melanoma cell lines with wildtype p16 (Figure 3A). Consistent with our data in fibroblasts (Figures 1, 2), knockdown of p16 in the melanoma cells also decreased *IL6* and *CXCL8* (Figure 3B–3D). Notably, this was not a consequence of a reduced burden of spontaneous senescent cells in p16 knockdown cells (Supplementary Figure 3A, 3B). Finally, expression of *IL6* and *CXCL8* was also significantly reduced by stable knockdown of p16 in melanoma cells induced to senesce using etoposide (Figure 3E–3H). Etoposide induced senescence to a similar extent in both p16 wildtype controls and p16 knockdown cells, suggesting the decrease in expression was not linked to decreased senescence (Figure 3E–3G). Altogether, these data suggest that p16 may directly or indirectly regulate the transcription of both *IL6* and *CXCL8* and support the hypothesis that this is not a consequence of p16 suppression-mediated senescence bypass since suppression of p16 in both senescent and proliferating melanoma cells abrogates *IL6* and *CXCL8*.

Low *CDKN2A* in patient tumors correlates with low SASP expression

It has been widely demonstrated that suppression of p16 leads to increased proliferation, tumorigenesis, and metastasis *in vitro* and *in vivo*, and loss of p16 expression is considered a poor prognostic maker [66–69]. To further understand the relationship between loss of p16 and decreased expression of the SASP, we used TCGA data from primary tumors of skin cutaneous melanoma (SKCM, n=103), pancreatic adenocarcinoma

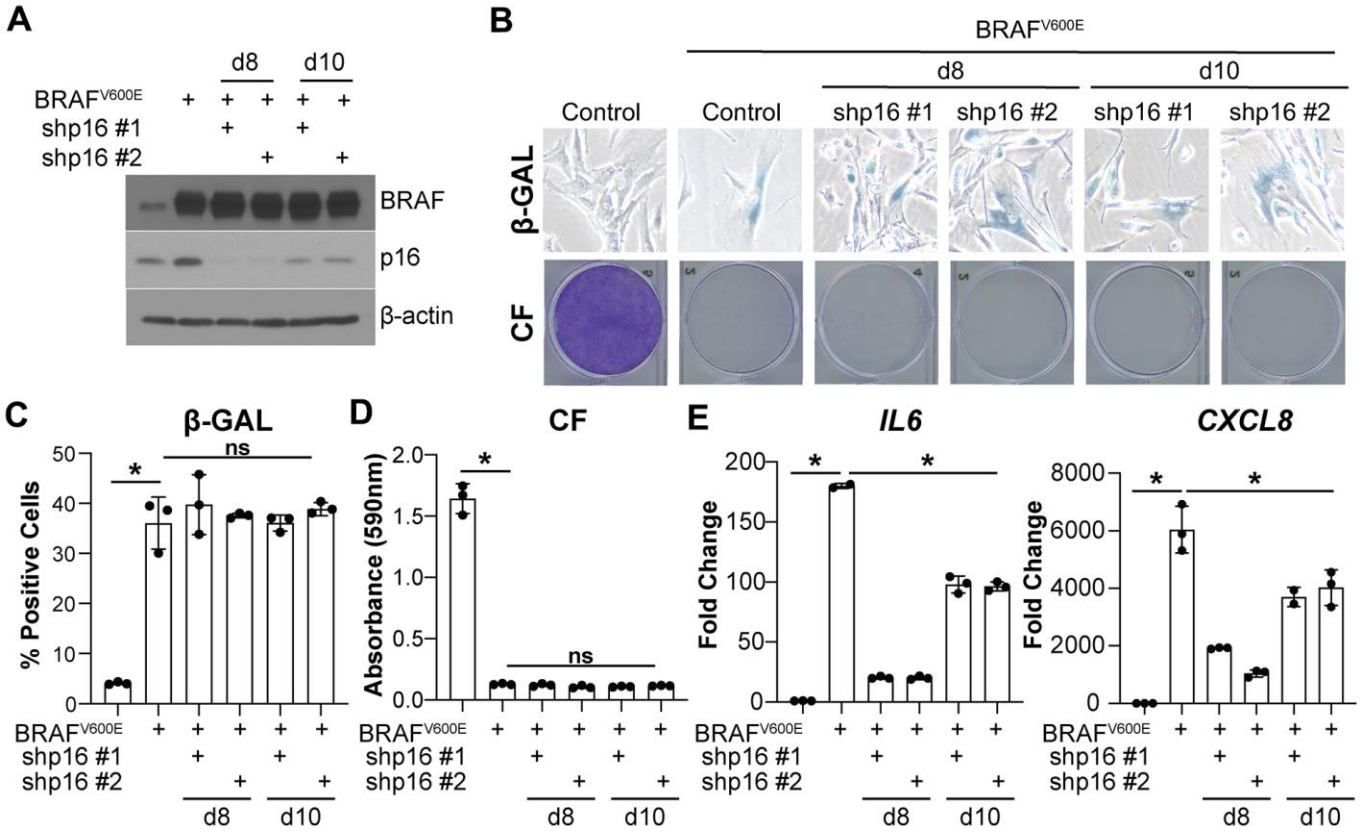

Figure 2. Knockdown of p16 at later timepoints decreases *IL6* and *CXCL8* expression without bypassing oncogene-induced senescence. IMR90s expressing BRAF^{V600E} alone or in combination with shRNAs targeting p16 (shp16 hairpin #1 and #2). An empty pBabe retroviral vector and a shRNA targeting GFP lentiviral vector were used as controls. See Supplementary Figure 2A for an experimental timeline. (**A**) Immunoblot of BRAF and p16. β-actin was used as loading control. (**B**) Representative images of senescence-associated β-galactosidase (β-GAL) staining and colony formation (CF). (**C**) Quantification of β-GAL in (**B**). (**D**) Quantification of CF in (**B**). (**E**) *IL6* and *CXCL8* mRNA expression (fold change relative to control mean). Expression of target genes was normalized against multiple reference genes. Data normalized against *PMSC4* are shown. n=3/group and mean±SD. 1 out of 3 experiments is shown. *p<0.05. ns = not significant.

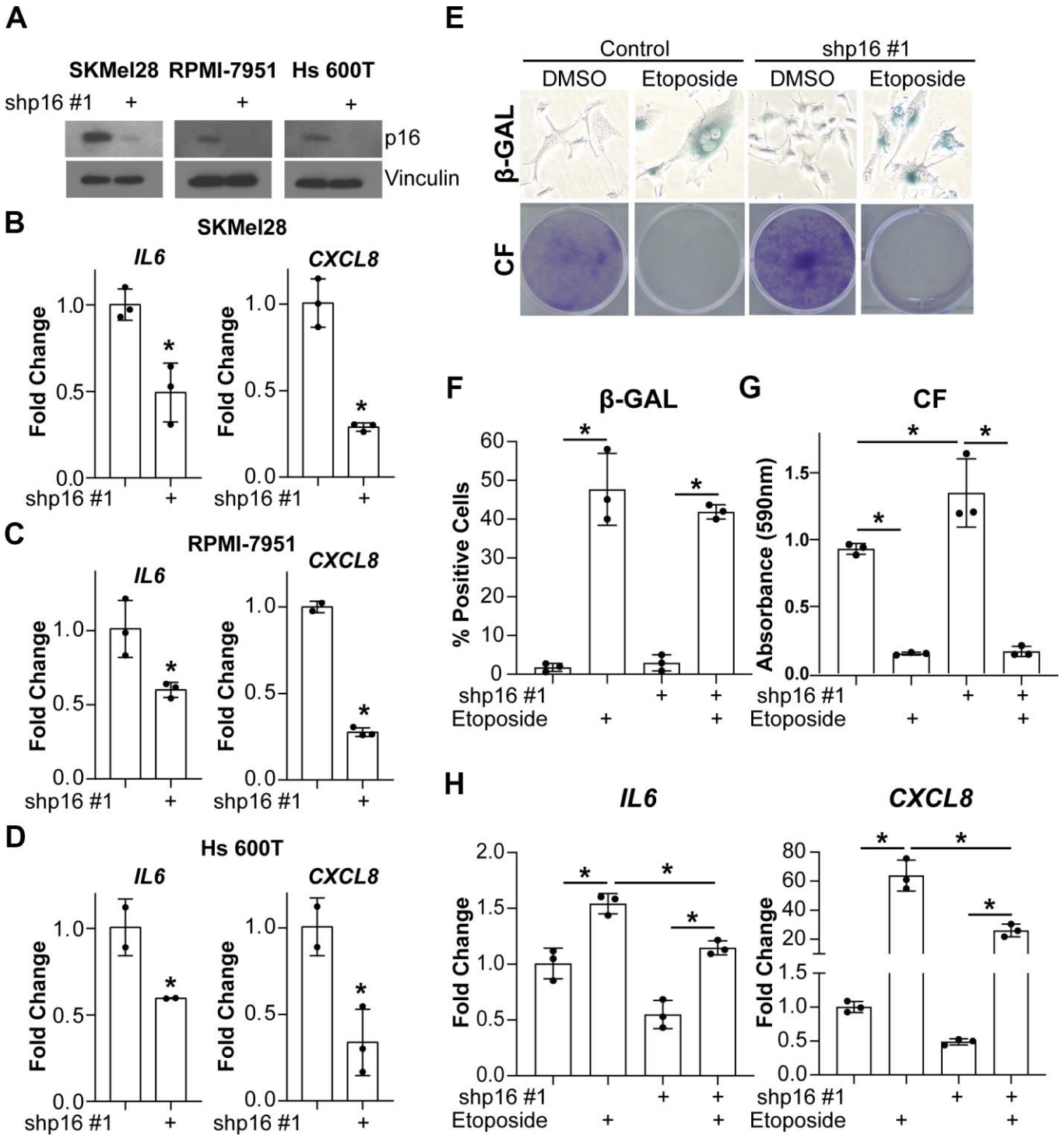

Figure 3. Knockdown of p16 in melanoma cells decreases *IL6* and CXCL8 expression. The melanoma cell lines SKMel28, RPMI-7951, and Hs 600T expressing wildtype p16 were infected with lentivirus expressing a shRNA targeting p16 (shp16 hairpin #1). An shRNA targeting GFP lentiviral vector was used as control. (**A**) Immunoblot of p16. Vinculin was used as loading control. (**B**–**D**) mRNA expression of *IL6* and *CXCL8* (fold change relative to control mean) in SKMel28 (**B**), RPMI-7951 (**C**), and Hs 600T (**D**) melanoma cells. Expression of target genes was normalized against multiple reference genes. Data normalized against *MRPL9* are shown. n=3/group and mean±SD. 1 out of 3 experiments is shown. (**E**–**H**) p16 was stably knocked down in SKMel28 melanoma cells with a shRNA (shp16 hairpin #1). An shRNA targeting GFP lentiviral vector was used as control. Cells were treated with 1μM etoposide for 6 days. (**E**) Representative images of senescence-associated β-galactosidase (β-GAL) staining and colony formation (CF). (**F**) Quantification of β-GAL in (**E**). (**G**) Quantification of CF in (**E**). (**H**) *IL6* and *CXCL8* mRNA expression (fold change relative to control mean). Expression of target genes was normalized against multiple reference genes. Data normalized against *PMSC4* are shown. n=3/group and mean±SD. 1 out of 2 experiments is shown. *p<0.05.

(PAAD, n=178), colorectal adenocarcinoma (COADREAD, n=622), mesothelioma (MESO, n=87), bladder urothelial carcinoma (BLCA, n=407) and glioblastoma multiforme (GBM, n=153), six tumor types where loss of p16 is frequently observed and has clinical implications [70–77]. Patients were classified according to their *CDKN2A* status (p16-low or p16-high, see Methods for details) (Table 1), and differential expression analysis was performed independently for each tumor type. Note that there were no significant differences in the number of normal and tumor cells between p16-high and p16-low tumors (Supplementary Figure 4A). Most of the SASP factors profiled in a published database of RAS-induced senescence (including soluble factors and exosomes, 232 total unique genes) (Supplementary Table 1) [54], were significantly downregulated in p16-low tumors (Supplementary Figure 4A and Supplementary Table 2). Gene Set Enrichment Analysis (GSEA) also showed a decrease in 'Senescence Associated Secretory Phenotype, SASP' (Figure 4B) in p16-low tumors. Interestingly, 4 out of 6 tumors (PAAD, COADREAD, MESO, and BLCA) showed a decrease in pathways related to inflammation and the immune system such as 'Antigen Processing and Presentation' and 'Cytosolic DNA Sensing Pathway' in p16-low tumors (Supplementary Figure 4B). These data demonstrate that p16 status correlates with expression of SASP factors in human tumor samples. Importantly, to rule out the possibility of less senescent tumor cells in the p16-low patient samples, we used GSEA to cross-compare p16-low vs. p16-high expression profiles with a previously published senescence expression signature [78]. Among the 6 tumor types, only MESO showed a significant negative normalized enrichment score (NES) (Supplementary Table 3). This suggests that in 5 of the 6 tumor types, there was not a significant decrease in the number of intratumoral-senescent cells. Thus, the observed decrease in SASP expression signatures is likely not due to less intratumoral senescent cells. To unravel whether this observation is due to a decrease of immune cell infiltration in p16-low vs. p16-high tumors, we compared the number of infiltrating lymphocytes, monocytes, and neutrophils seen on OCT-embedded tissue slides reported by TCGA in 5 out of 6 tumors (note that there is no available data for GBM). No significant differences were observed between p16-low and p16-high tumors (Supplementary Figure 4C). These data at least in part suggest that changes in SASP expression are not due to differences in intratumoral senescent cells or differential infiltration of immune cells that could potentially bias our analysis.

Finally, since we observed a downregulation of the "Cytosolic DNA Sensing Pathway" signature, we correlated the expression level of *CDKN2A* and *LMNB1* in the tumors. We did not observe a strong correlation between *CDKN2A* and *LMNB1* expression (Figure 4C), suggesting that p16 regulation of this pathway and the SASP in tumors may not be directly through modulation of *LMNB1*. However, we cannot rule out the possibility that other pathways may be altered to affect the cytosolic DNA sensing pathway. All together with our *in vitro* data, these data in human tumor samples demonstrate a universal, positive correlation between p16 expression and SASP gene expression.

DISCUSSION

Increased expression of p16 and the SASP are characteristics of OIS; however, the relationship between them is not well understood. While increased p16 expression has a clear role in sustaining the characteristic cell cycle arrest of OIS cells [8, 79], the SASP appears to be a consequence of the DNA damage response induced by OIS and is not necessary for the proliferative arrest [24, 80, 81]. Indeed, this is evident by the observation that p16-mediated senescence induction, a stimulus that a priori only restrains cell cycle progression, does not induce SASP expression [60]. Here we found that knockdown p16 decreases gene expression of two of the most well characterized SASP factors *IL6* and *CXCL8* [13, 16, 61], in a manner that is uncoupled from senescence bypass (Figures 1, 2). Knockdown of p16 or low expression of *CDKN2A* in patient tumors was also associated with lower expression of additional SASP factors. Together, this suggests that p16 expression is not sufficient but is necessary to induce expression of the SASP.

One important question that remains is how does p16 loss mechanistically affect SASP gene expression? p16 is a critical cell cycle regulator, and its suppression both enhances proliferation and allows for senescence bypass [8–10, 12, 82, 83]. Decreased *LMNB1* expression plays an important role in the establishment of the SASP [84]. Recent publications demonstrate that decreased expression of *LMNB1* and the consequential decrease of nuclear integrity leads to the accumulation of cytoplasmic chromatin fragments (CCFs) that in turn activate the cGAS-STING signaling pathway to drive the SASP [36–38, 85, 86]. Importantly, we found that knockdown of p16 decreased SASP gene expression, which was not a consequence of increased *LMNB1* expression (Figure 2). These data suggest that the observed changes in SASP gene expression are not due to downregulation of cGAS-STING signaling, which is directly affected by *LMNB1* and nuclear integrity [36]. Notably, we found that four out of the six tumor types analyzed here have decreased cytosolic DNA sensing pathway signaling in p16-low vs. p16-high tumors (Supplementary Figure 4B); however, no correlation

Table 1. Statistics of TCGA data sets.

	SKCM	PAAD	COADREAD	MESO	BLCA	GBM
Total cases	103	178	622	87	407	153
***CDKN2A* expression (Log_2RSEM) mean**	7.08	6.73	6.31	6.25	7.56	6.61
***CDKN2A* expression (Log_2RSEM) standard deviation (SD)**	2.76	2.32	1.74	2.26	3.61	3.15
***CDKN2A* expression (Log_2RSEM) median**	7.75	6.35	6.22	6.29	8.22	5.11
***CDKN2A* expression (Log_2RSEM) first quartile (Q_1)**	5.15	4.93	5.20	4.59	4.16	4.07
***CDKN2A* expression (Log_2RSEM) third quartile (Q_3)**	9.02	8.38	7.30	7.68	10.82	10.40
No. p16-low cases (*CDKN2A* expression ≤ Q_1)	103	45	156	22	102	38
No. p16-high cases (*CDKN2A* expression ≥ Q_3)	103	45	156	22	102	38

was found between *CDKN2A* and *LMNB1* mRNA expression (Figure 4C), suggesting that additional mechanisms are at play in tumors with low p16 expression. It is important to note that besides loss of nuclear integrity, there are other phenomena (mitochondrial DNA leakage, upregulation of LINE-1, or increased expression of the endonuclease MUS81) that may contribute to an impaired cytosolic DNA sensing pathway (reviewed in [87]). Loss of *CDKN2A* is often due to deletion or hypermethylation of the locus [70]. Interestingly, previous work has suggested that melanomas with low *MTAP* have decreased cGAS-STING signaling [88], and *MTAP* is often co-deleted/silenced with *CDKN2A* [89]. Therefore, multiple mechanisms may exist in tumors with loss of this locus to suppress SASP gene expression and/or modulate the tumor microenvironment. Additionally, p16 can negatively regulate *TP53* (encoding for p53) at the transcriptional level and also at the protein level by increasing Mdm2-dependent degradation of p53 [90, 91]. As p53 is a negative regulator of the SASP [92], it is possible that the observed decrease in SASP expression upon p16 suppression is due to negative regulation of p53. Future studies are needed to determine the exact mechanism by which p16 suppression decreases SASP gene expression. Moreover, determining whether these transcription changes in SASP gene expression are a direct or indirect effect of low p16 expression will be of great importance.

We and others have shown that in addition to its canonical role regulating cell cycle progression though the RB pathway, p16 has non-canonical activities that regulate other important aspects of cellular physiology such as nucleotide metabolism, reactive oxygen species, and miRNAs among others [93, 94]. In this regard, some studies have found that pharmacological inhibition of canonical downstream targets of p16, namely CDK4/6, leads to an induction of SASP factors, recruitment of antitumor immune cells, and senescence [95–98], suggesting that p16-loss-mediated regulation of SASP expression and the tumor immune microenvironment may be due to non-canonical (RB-independent) mechanisms. On the contrary, other authors suggest that inhibition of CDK4/6 alone does not induce a SASP and immunologic responses [99]. Additional studies are needed to delineate the exact mechanism whereby suppression of p16 decreases SASP and verify that this occurs in an RB-independent, non-canonical pathway.

Our data suggest that multiple tumor types with low *CDKN2A* (i.e., p16-low) expression have decreased SASP factor expression (Figure 4). A potential caveat of our study is that the SASP factor list we have used for our analysis is broad, and some factors are related to secretion in exosomes [54]. Use of a broad, validated list of SASP factors, while imperfect, allowed us to analyze the TCGA data in a more unbiased fashion versus manually curating a list. Additionally, we demonstrated that knockdown of p16 in $BRAF^{V600E}$-induced senescence *in vitro* corresponds with a decrease in different SASP factors including inflammatory factors, growth factors, metalloproteinases, and ligands (Figure 1I, 1J and Supplementary Figure 1I). Nonetheless, our study shows that low *CDKN2A* expression correlates with downregulation of a distinctive SASP profile depending on the tissue of origin (Figure 4A and Supplementary Table 2). This observation is consistent with previous studies suggesting that the SASP composition is temporally

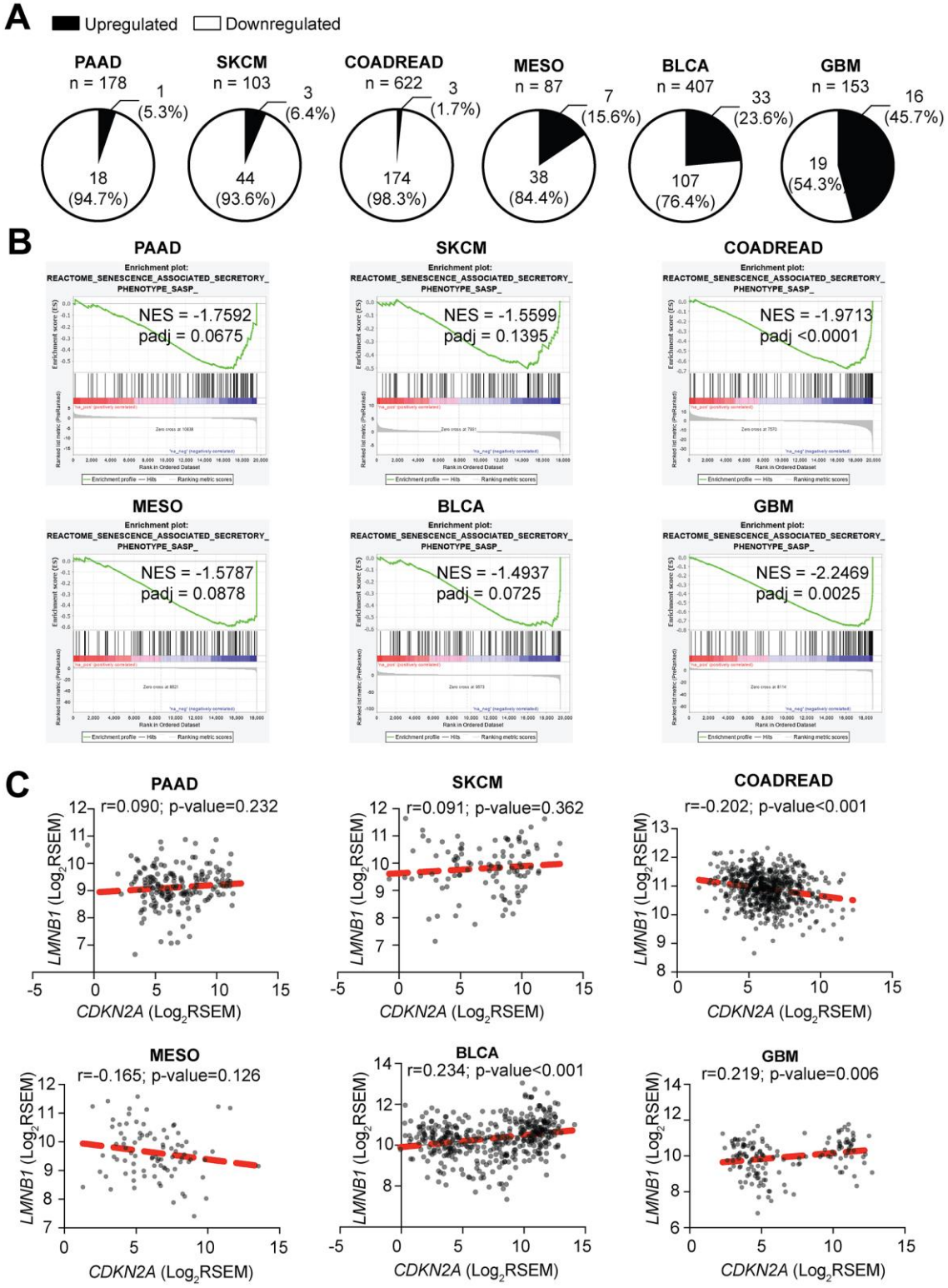

Figure 4. Tumors with low *CDKN2A* expression have decreased expression of SASP. (**A**) Percentage of SASP genes significantly upregulated and downregulated in *CDKN2A*-low (i.e., p16-low) expressing tumors when compared to *CDKN2A*-high (i.e., p16-high) expressing tumors. (**B**) Negatively enriched SASP term among the six studied tumor types in Gene Set Enrichment Analysis (GSEA) between *CDKN2A*-low and *CDKN2A*-high expressing tumors. SKCM (skin cutaneous melanoma), PAAD (pancreatic adenocarcinoma), COADREAD (colorectal adenocarcinoma), MESO (mesothelioma), BLCA (bladder urothelial carcinoma), GBM (glioblastoma multiforme), NES (negative enrichment score). (**C**) Correlation between *CDKN2A* and *LMNB1* expression for each tumor type. Data are shown as Log_2 of RSEM. Coefficient of correlation (r) and p-value were calculated using Pearson's correlation.

dynamic and context- and senescence inducer-dependent [54, 55, 100]. Characterization of the different SASP profiles and their unique dynamics will be critical not only to assess the senescent cell burden, but also to develop specific and personalized senescence- and SASP-targeted therapies. Moreover, it will be important to determine whether these tumor-specific SASP signatures alter the clinical course of each tumor type or response to therapy. This study is focused on the transcriptional expression regulation of the SASP upon loss of p16; however, additional studies investigating whether these findings impact the translation and secretion of the SASP, especially within exosomes, are warranted. Since suppression of p16 can lead to senescence bypass and promote tumorigenesis [8–10, 12, 82, 83], obtaining profiles of the SASP factors related to this process may help treat the ~50% of all human tumors with low p16 expression [59].

It is well-established that the SASP has pleiotropic, context-dependent effects that both promote tumor progression, but also enhance anti-tumor immunity (reviewed in [101]). For example, IL6 promotes chronic inflammation and tumorigenesis [102]. However, recent studies suggest that IL6 can also enhance anti-tumor immunity by resculpting T cell-mediated immune responses [102]. Likewise, other SASP factors, such as IL1a, IL1b, and TNF have this dual role where they can both promote inflammation and tumorigenesis or impair malignant transformation of benign nevi [103]. Using data from TCGA, we found decreased 'Antigen Processing and Presentation' signaling [i.e., the ability of antigen presenting cells to present antigens on major histocompatibility complexes (MHCs) to T-cells] in some patients with low *CDKN2A* expression (Supplementary Figure 4B). Consistent with our observation, it has been shown that OIS primary human melanocytes upregulate the MHC class II apparatus to induce T-cell proliferation and that melanoma patients that sustain this feature have a favorable disease outcome [104]. Additionally, suppression of p16 activity has been associated with immune deserts, immune escape, and low cytolytic activity in melanoma and pancreatic adenocarcinoma [105–107]. Thus, it is possible that in the context of certain tumor types such as those studied here, the decreased expression of SASP factors observed upon p16 knockdown or in *CDKN2A*-low patients may contribute to abrogation of senescence surveillance by immune cells [48, 108], thereby promoting tumorigenesis. Interestingly, a recent publication shows that depletion of p16 in tumor cells abrogates the cancer immune response and promotes immune checkpoint blockade resistance [109]. Here, we did not observe a difference in immune cell infiltration between p16-low and p16-high patient samples (Supplementary Figure 4C), which may suggest that the activity of the immune cells is altered. Future experiments will determine whether suppression of p16 leads to decreased immune surveillance and the mechanism whereby this occurs.

Although loss of p16 is one of the most common events in cancer (~50% of all human cancers), there are currently no approved targeted therapies [93]. Additionally, we and others have shown that suppression of p16 has roles outside the cell cycle that would not be affected with current therapies undergoing clinical trials targeting CDK4/6 [93]. Therefore, finding downstream targetable pathways may be beneficial for this large subset of patients. For instance, we previously showed that inhibition of nucleotide metabolism through suppression of mTORC1 or the pentose phosphate pathway enzyme Ribose 5-Phosphate Isomerase A (RPIA) induces senescence specifically in p16-low cancers [8]. Here we found that suppression of p16 leads to decreased SASP expression. Therefore, induction of senescence in p16-low cancers may be a valuable strategy to inhibit the cell cycle while not activating the potential deleterious effects of the SASP.

In summary, we found that suppression of p16 decreases expression of multiple SASP genes, which cannot be explained by inhibition of senescence. We found that this phenomenon also occurs in p16-wildtype tumor cells upon p16 knockdown, and there is a decrease in the SASP gene signature in multiple tumor types that are associated with low p16 expression. Understanding whether p16 regulates SASP expression is critical to understand the complex relationship between cellular senescence, the immune system, and the cell cycle, three key players in cancer regulation.

MATERIALS AND METHODS

Cell lines

Normal diploid IMR90 human fibroblasts were obtained from ATCC (CCL-186) and cultured according to the ATCC protocol in DMEM (Corning, cat#10-017-CV) supplemented with 5% FBS (VWR, cat#97068-085), L-glutamine (Corning, cat#25-015-CI), non-essential amino acids (Corning, cat#25-025-CI), sodium pyruvate (Corning, cat#25-000-CI), and sodium bicarbonate (Corning, cat#25-035-CI). Cells were cultured under physiological oxygen conditions (2% O_2) and 5% CO_2. Normal skin fibroblasts derived from a melanoma patient Hs 895.Sk were obtained from ATCC (CRL-7636) and cultured in DMEM (Corning, cat#10-013-CV) supplemented with 10% FBS (VWR, cat#97068-085). Experiments were performed on IMR90 between population doubling #25-35 and in Hs 895.Sk between population doubling #4-10. Melanoma cell lines

SKMel28, Hs 600.T, and RPMI-7951, were obtained from ATCC (HTB-72, CRL-7368, and HTB-66, respectively). SKMel28 and Hs 600.T as well as the lentiviral and retroviral packaging cells (293FT and Phoenix, respectively) were cultured in DMEM (Corning, cat#10-013-CV) supplemented with 10% FBS, while RPMI-7951 were cultured in EMEM (ATCC, cat#30-2003) supplemented with 10% FBS. Hs 895.Sk and cancer cell lines were cultured under atmospheric oxygen (~20%) and 5% CO_2. All cell lines were cultured in MycoZap (Lonza, cat#VZA-2032) and were tested for mycoplasma every two months as described in [110]. All tumor cell lines express wildtype *CDKN2A* according to TCGA [111, 112].

Lentiviral and retroviral packaging and infection

pBabe $BRAF^{V600E}$ (Addgene cat#15269), pBabe $HRAS^{G12V}$ (Addgene cat#9051), and pBabe empty control (Addgene cat#1764) vectors were packaged into retroviral particles using the BBS/calcium chloride method as previously described in [8]. pLKO.1-shp16 #1 (TRCN0000010482), pLKO.1-shp16 #2 (TRCN0000039751), and pLKO.1-shGFP control (Addgene, cat#30323) vectors were packaged using the ViraPower Kit (Invitrogen, cat# K497500). Experimental timelines for IMR90 and Hs 895.Sk are delineated in Supplementary Figure 1A and Supplementary Figure 2A. Briefly, cells were infected with pBabe empty vector control, pBabe $BRAF^{V600E}$, or pBabe $HRAS^{G12V}$ retroviral particles, and 24 hours later cells were infected with a second round of corresponding retroviral particles. Cells were infected with pLKO.1-shp16 or pLKO.1-shGFP when indicated in Supplementary Figure 1A and Supplementary Figure 2A. As noted in Figure Legends, empty vector pBabe and/or pLKO.1-shGFP were used as controls for all experiments to limit possible effects from expression of viral vectors. Cells were selected with 1μg/mL puromycin for single infections or 3μg/mL for double infections until the end of the experimental procedure.

Etoposide-induced senescence

SKMel28 melanoma cells (p16-wildtype) with stable p16 knockdown (using shp16 hairpin #1) or control (shGFP) were treated with either DMSO or 1μM etoposide (Cayman Chemical, cat#12092) for 6 days (drug replacement every 2 days).

RT-qPCR

Total RNA was extracted from cells with Trizol (Ambion, cat#15596018) and DNase treated, cleaned, and concentrated using Zymo columns (Zymo Research, cat#R1013) following the manufacturer's instructions. Optical density values for RNA were measured using NanoDrop One (Thermo Scientific) to confirm an A260 and A280 ratios above 1.9. Relative expression of target genes was analyzed using the QuantStudio 3 Real-Time PCR System (Thermo Fisher Scientific) with clear 96-well plates (Greiner Bio-One, cat#652240). Primers were designed using the Integrated DNA Technologies (IDT) web tool (Supplementary Table 4). A total of 50ng of RNA was used for One-Step qPCR (Quanta BioSciences, cat# 95089-200) following the manufacturer's instructions in a final volume of 10μL. Conditions for amplification were: 10 min at 48° C, 5 min at 95° C, 40 cycles of 10 sec at 95° C and 7 sec at 62° C. The assay ended with a melting curve program: 15 sec at 95° C, 1 min at 70° C, then ramping to 95° C while continuously monitoring fluorescence. Each sample was assessed in triplicate. Relative quantification was determined to multiple reference genes (*MRPL19*, *PSMC4*, and *PUM1*) to ensure reproducibility using the delta-delta CT method.

Western blotting

Cell lysates were collected in 1X sample buffer (2% SDS, 10% glycerol, 0.01% bromophenol blue, 62.5mM Tris, pH=6.8, 0.1M DTT) and boiled (10 min, 95° C). Protein concentration was determined using Bradford assay (Bio-Rad, cat#5000006). Proteins were resolved using SDS-PAGE gels and transferred to nitrocellulose membranes (GE Healthcare Life Sciences, cat#10600001) as previously described [8]. Antibodies used include: anti-BRAF (Santa Cruz Biotechnology, cat#sc-5284, 1:1000), anti-RAS (BD Sciences, cat#610001, 1:1000), anti-p16 (Abcam, cat#ab108349, 1:1000), anti-p21 (Abcam cat#ab109199, 1:1000), anti-cyclin A2 (Abcam cat#ab181591, 1:2000), anti-vinculin (Sigma-Aldrich cat#V9131, 1:1000), β-Actin (Sigma-Aldrich, cat#A1978, 1:10000), anti-mouse HRP (Cell Signaling Technology, cat#cst7076, 1:10,000), and anti-rabbit HRP (Cell Signaling Technology, cat#cst7074, 1:5000).

Senescence and proliferation assays

SA-β-Gal staining was performed as previously described [113]. Cells were fixed in 2% formaldehyde/0.2% glutaraldehyde in PBS (5 min) and stained (40 mM Na_2HPO_4, 150 mM NaCl, 2 mM $MgCl_2$, 5mM$K_3Fe(CN)_6$, 5 mM $K_4Fe(CN)_6$, and 1 mg/ml X-gal) overnight at 37° C in a non-CO_2 incubator. Images were acquired at room temperature using an inverted microscope (Nikon Eclipse Ts2) with a 20X/0.40 objective (Nikon LWD) equipped with a camera (Nikon DS-Fi3). Each sample was assessed in triplicate and at least 100 cells per well were counted (>300 cells per experiment). For colony formation, an

equal number of cells were seeded in 6-well plates (for IMR90s) and 12-well plates (for SKMel28) and cultured for an additional 1-2 weeks. Colony formation was visualized by fixing cells in 1% paraformaldehyde (5 min) and staining with 0.05% crystal violet (20 min). Wells were de-stained in 500mL 10% acetic acid (10 min). Absorbance (590nm) was measured using a spectrophotometer (Spectra Max 190). Each sample was assessed in triplicate.

Differential expression analysis

Preprocessed and processed RNA-Seq data from primary tumors of skin cutaneous melanoma (SKCM), pancreatic adenocarcinoma (PAAD), colorectal adenocarcinoma (COADREAD), mesothelioma (MESO), bladder urothelial carcinoma (BLCA), and glioblastoma multiforme (GBM) TCGA data sets were downloaded from BROAD GDAC Firehose on June 22, 2020 (SKCM, COADREAD, and PAAD) and October 6, 2020 (MESO, BLCA, GBM) [Broad Institute TCGA Genome Data Analysis Center (2016): Firehose 2016_01_28 run. Broad Institute of MIT and Harvard. doi:10.7908/C11G0KM9)]. Processed rnaseqv2 files containing normalized RSEM expression values for each gene in each patient were used to determine the first and third quartile of *CDKN2A* expression for each tumor type separately (Table 1). Quartile values were used to classify patients into p16-low (*CDKN2A* expression ≤ Q1) and p16-high (*CDKN2A* expression ≥ Q3) groups. Differential expression analysis between p16-low and p16-high patients for each tumor type was performed using the preprocessed raw-counts files in R-CRAN (R-3.6.3) and the DESeq2 package.

Gene set enrichment analysis (GSEA)

Genes were ranked according to the fold-change and p-value obtained in the differential expression analysis between p16-low vs. p16-high as follows: $-\log_{10}$(p-value) x sign ($\log_2$ fold change). Pre-ranked files were built for each tumor type separately in R-CRAN (R-3.6.3) and used to run pre-ranked GSEA (javaGSEA desktop application) for KEGG and Reactome under predefined parameters (1000 permutations, weighted enrichment statistic, excluding sets larger than 500 and smaller than 15 and using meandiv normalization mode, there were no repeated genes thus collapse mode was not used). Following GSEA documentation indications, terms were considered significant when the FDR adjusted p-value (q-value) was <0.25 (http://software.broadinstitute.org/gsea/index.jsp). Gene sets for "Casella et al. senescence upregulated genes" (50 genes) and "Casella et al. senescence downregulated genes" (18 genes) were built in GMX files from publicly-available expression senescence signatures [78] and used to run GSEA using previously described pre-ranked files and parameters.

Statistical analysis

GraphPad Prism version 7.0 was used to perform statistical analysis. The level of significance between two groups was assessed with unpaired t test. For data sets with more than two groups, one-way ANOVA followed by Tukey's post hoc test was applied. P-values< 0.05 were considered significant. Pearson correlation test in GraphPad Prism version 7.0 was used to assess the correlation between *LMNB1* and *CDKN2A*. The percentages of normal and tumor cells as well as tumor infiltrating lymphocytes, monocytes, and neutrophils for TCGA tumors were obtained from the biospecimen file at BROAD GDAC Firehose on October 6, 2020.

AUTHOR CONTRIBUTIONS

R.B. and K.M.A. designed the experiments; R.B., K.E.L., and M.A.A. conducted the experiments; R.B. performed data analysis; R.B. and K.M.A. wrote the manuscript. All authors contributed to editing the manuscript.

ACKNOWLEDGMENTS

We thank Drs. Erika Dahl, Chi-Wei Chen, and Naveen Kumar Tangudu for critical reading and editing of this manuscript. We also thank Dr. Gary Nolan from Stanford University for providing with Phoenix packaging cells.

CONFLICTS OF INTEREST

The authors declare that they have no conflicts of interest.

FUNDING

This work was supported by grants from the National Institutes of Health (F31CA250366 to K.E.L. and R37CA240625 and R00CA194309 to K.M.A.) and a Penn State Cancer Institute Postdoctoral Fellowship (R.B.).

REFERENCES

1. Collado M, Blasco MA, Serrano M. Cellular senescence in cancer and aging. Cell. 2007; 130:223–33. https://doi.org/10.1016/j.cell.2007.07.003 PMID:17662938

2. Aird KM, Zhang R. Nucleotide metabolism, oncogene-induced senescence and cancer. Cancer Lett. 2015; 356:204–10.

https://doi.org/10.1016/j.canlet.2014.01.017 PMID:24486217

3. Yaswen P, Campisi J. Oncogene-induced senescence pathways weave an intricate tapestry. Cell. 2007; 128:233–34. https://doi.org/10.1016/j.cell.2007.01.005 PMID:17254959

4. Bringold F, Serrano M. Tumor suppressors and oncogenes in cellular senescence. Exp Gerontol. 2000; 35:317–29. https://doi.org/10.1016/s0531-5565(00)00083-8 PMID:10832053

5. Serrano M, Lin AW, McCurrach ME, Beach D, Lowe SW. Oncogenic ras provokes premature cell senescence associated with accumulation of p53 and p16INK4a. Cell. 1997; 88:593–602. https://doi.org/10.1016/s0092-8674(00)81902-9 PMID:9054499

6. Stein GH, Drullinger LF, Soulard A, Dulić V. Differential roles for cyclin-dependent kinase inhibitors p21 and p16 in the mechanisms of senescence and differentiation in human fibroblasts. Mol Cell Biol. 1999; 19:2109–17. https://doi.org/10.1128/mcb.19.3.2109 PMID:10022898

7. Sherr CJ. The INK4a/ARF network in tumour suppression. Nat Rev Mol Cell Biol. 2001; 2:731–37. https://doi.org/10.1038/35096061 PMID:11584300

8. Buj R, Chen CW, Dahl ES, Leon KE, Kuskovsky R, Maglakelidze N, Navaratnarajah M, Zhang G, Doan MT, Jiang H, Zaleski M, Kutzler L, Lacko H, et al. Suppression of p16 induces mTORC1-mediated nucleotide metabolic reprogramming. Cell Rep. 2019; 28:1971–80.e8. https://doi.org/10.1016/j.celrep.2019.07.084 PMID:31433975

9. Chin L, Pomerantz J, Polsky D, Jacobson M, Cohen C, Cordon-Cardo C, Horner JW 2nd, DePinho RA. Cooperative effects of INK4a and ras in melanoma susceptibility *in vivo*. Genes Dev. 1997; 11:2822–34. https://doi.org/10.1101/gad.11.21.2822 PMID:9353252

10. Dankort D, Filenova E, Collado M, Serrano M, Jones K, McMahon M. A new mouse model to explore the initiation, progression, and therapy of BRAFV600E-induced lung tumors. Genes Dev. 2007; 21:379–84. https://doi.org/10.1101/gad.1516407 PMID:17299132

11. Goel VK, Ibrahim N, Jiang G, Singhal M, Fee S, Flotte T, Westmoreland S, Haluska FS, Hinds PW, Haluska FG. Melanocytic nevus-like hyperplasia and melanoma in transgenic BRAFV600E mice. Oncogene. 2009; 28:2289–98. https://doi.org/10.1038/onc.2009.95 PMID:19398955

12. Haferkamp S, Becker TM, Scurr LL, Kefford RF, Rizos H. p16INK4a-induced senescence is disabled by melanoma-associated mutations. Aging Cell. 2008; 7:733–45. https://doi.org/10.1111/j.1474-9726.2008.00422.x PMID:18843795

13. Coppé JP, Desprez PY, Krtolica A, Campisi J. The senescence-associated secretory phenotype: the dark side of tumor suppression. Annu Rev Pathol. 2010; 5:99–118. https://doi.org/10.1146/annurev-pathol-121808-102144 PMID:20078217

14. Acosta JC, Banito A, Wuestefeld T, Georgilis A, Janich P, Morton JP, Athineos D, Kang TW, Lasitschka F, Andrulis M, Pascual G, Morris KJ, Khan S, et al. A complex secretory program orchestrated by the inflammasome controls paracrine senescence. Nat Cell Biol. 2013; 15:978–90. https://doi.org/10.1038/ncb2784 PMID:23770676

15. Baker DJ, Wijshake T, Tchkonia T, LeBrasseur NK, Childs BG, van de Sluis B, Kirkland JL, van Deursen JM. Clearance of p16Ink4a-positive senescent cells delays ageing-associated disorders. Nature. 2011; 479:232–36. https://doi.org/10.1038/nature10600 PMID:22048312

16. Coppé JP, Patil CK, Rodier F, Sun Y, Muñoz DP, Goldstein J, Nelson PS, Desprez PY, Campisi J. Senescence-associated secretory phenotypes reveal cell-nonautonomous functions of oncogenic RAS and the p53 tumor suppressor. PLoS Biol. 2008; 6:2853–68. https://doi.org/10.1371/journal.pbio.0060301 PMID:19053174

17. Laberge RM, Sun Y, Orjalo AV, Patil CK, Freund A, Zhou L, Curran SC, Davalos AR, Wilson-Edell KA, Liu S, Limbad C, Demaria M, Li P, et al. MTOR regulates the pro-tumorigenic senescence-associated secretory phenotype by promoting IL1A translation. Nat Cell Biol. 2015; 17:1049–61. https://doi.org/10.1038/ncb3195 PMID:26147250

18. Takasugi M, Okada R, Takahashi A, Virya Chen D, Watanabe S, Hara E. Small extracellular vesicles secreted from senescent cells promote cancer cell proliferation through EphA2. Nat Commun. 2017; 8:15729. https://doi.org/10.1038/ncomms15728 PMID:28585531

19. Acosta JC, O'Loghlen A, Banito A, Guijarro MV, Augert A, Raguz S, Fumagalli M, Da Costa M, Brown C, Popov

N, Takatsu Y, Melamed J, d'Adda di Fagagna F, et al. Chemokine signaling via the CXCR2 receptor reinforces senescence. Cell. 2008; 133:1006–18. https://doi.org/10.1016/j.cell.2008.03.038 PMID:18555777

20. Freund A, Patil CK, Campisi J. p38MAPK is a novel DNA damage response-independent regulator of the senescence-associated secretory phenotype. EMBO J. 2011; 30:1536–48. https://doi.org/10.1038/emboj.2011.69 PMID:21399611

21. Kang C, Xu Q, Martin TD, Li MZ, Demaria M, Aron L, Lu T, Yankner BA, Campisi J, Elledge SJ. The DNA damage response induces inflammation and senescence by inhibiting autophagy of GATA4. Science. 2015; 349:aaa5612. https://doi.org/10.1126/science.aaa5612 PMID:26404840

22. Kuilman T, Michaloglou C, Vredeveld LC, Douma S, van Doorn R, Desmet CJ, Aarden LA, Mooi WJ, Peeper DS. Oncogene-induced senescence relayed by an interleukin-dependent inflammatory network. Cell. 2008; 133:1019–31. https://doi.org/10.1016/j.cell.2008.03.039 PMID:18555778

23. Malaquin N, Olivier MA, Martinez A, Nadeau S, Sawchyn C, Coppé JP, Cardin G, Mallette FA, Campisi J, Rodier F. Non-canonical ATM/MRN activities temporally define the senescence secretory program. EMBO Rep. 2020; 21:e50718. https://doi.org/10.15252/embr.202050718 PMID:32785991

24. Rodier F, Coppé JP, Patil CK, Hoeijmakers WA, Muñoz DP, Raza SR, Freund A, Campeau E, Davalos AR, Campisi J. Persistent DNA damage signalling triggers senescence-associated inflammatory cytokine secretion. Nat Cell Biol. 2009; 11:973–79. https://doi.org/10.1038/ncb1909 PMID:19597488

25. Zhao J, Zhang L, Lu A, Han Y, Colangelo D, Bukata C, Scibetta A, Yousefzadeh MJ, Li X, Gurkar AU, McGowan SJ, Angelini L, O'Kelly R, et al. ATM is a key driver of NF-κB-dependent DNA-damage-induced senescence, stem cell dysfunction and aging. Aging (Albany NY). 2020; 12:4688–710. https://doi.org/10.18632/aging.102863 PMID:32201398

26. Aird KM, Iwasaki O, Kossenkov AV, Tanizawa H, Fatkhutdinov N, Bitler BG, Le L, Alicea G, Yang TL, Johnson FB, Noma KI, Zhang R. HMGB2 orchestrates the chromatin landscape of senescence-associated secretory phenotype gene loci. J Cell Biol. 2016; 215:325–34. https://doi.org/10.1083/jcb.201608026 PMID:27799366

27. Capell BC, Drake AM, Zhu J, Shah PP, Dou Z, Dorsey J, Simola DF, Donahue G, Sammons M, Rai TS, Natale C, Ridky TW, Adams PD, Berger SL. MLL1 is essential for the senescence-associated secretory phenotype. Genes Dev. 2016; 30:321–36. https://doi.org/10.1101/gad.271882.115 PMID:26833731

28. Chen H, Ruiz PD, McKimpson WM, Novikov L, Kitsis RN, Gamble MJ. MacroH2A1 and ATM play opposing roles in paracrine senescence and the senescence-associated secretory phenotype. Mol Cell. 2015; 59:719–31. https://doi.org/10.1016/j.molcel.2015.07.011 PMID:26300260

29. Hayakawa T, Iwai M, Aoki S, Takimoto K, Maruyama M, Maruyama W, Motoyama N. SIRT1 suppresses the senescence-associated secretory phenotype through epigenetic gene regulation. PLoS One. 2015; 10:e0116480. https://doi.org/10.1371/journal.pone.0116480 PMID:25635860

30. Leon KE, Aird KM. Jumonji C demethylases in cellular senescence. Genes (Basel). 2019; 10:33. https://doi.org/10.3390/genes10010033 PMID:30634491

31. Zhang B, Long Q, Wu S, Song S, Xu Q, Han L, Qian M, Ren X, Jiang J, Fu Q, Guo J, Zhang X, Chang X, et al. KDM4 Orchestrates Epigenomic Remodeling of Senescent Cells and Potentiates the Senescence-Associated Secretory Phenotype. bioRxiv. 2020. https://doi.org/10.1101/2020.08.03.235465

32. Leon KE, Buj R, Lesko E, Dahl ES, Chen C-W, Imamura Y, Kossenkov AV, Hobbs RP, Aird KM. DOT1L modulates the senescence-associated secretory phenotype through epigenetic regulation of IL1A. bioRxiv. 2020. https://doi.org/10.1101/2020.08.21.258020

33. Herranz N, Gallage S, Mellone M, Wuestefeld T, Klotz S, Hanley CJ, Raguz S, Acosta JC, Innes AJ, Banito A, Georgilis A, Montoya A, Wolter K, et al. mTOR regulates MAPKAPK2 translation to control the senescence-associated secretory phenotype. Nat Cell Biol. 2015; 17:1205–17. https://doi.org/10.1038/ncb3225 PMID:26280535

34. Freund A, Laberge RM, Demaria M, Campisi J. Lamin B1 loss is a senescence-associated biomarker. Mol Biol Cell. 2012; 23:2066–75. https://doi.org/10.1091/mbc.E11-10-0884 PMID:22496421

35. Shimi T, Butin-Israeli V, Adam SA, Hamanaka RB, Goldman AE, Lucas CA, Shumaker DK, Kosak ST, Chandel NS, Goldman RD. The role of nuclear lamin B1

in cell proliferation and senescence. Genes Dev. 2011; 25:2579–93.
https://doi.org/10.1101/gad.179515.111
PMID:22155925

36. Dou Z, Ghosh K, Vizioli MG, Zhu J, Sen P, Wangensteen KJ, Simithy J, Lan Y, Lin Y, Zhou Z, Capell BC, Xu C, Xu M, et al. Cytoplasmic chromatin triggers inflammation in senescence and cancer. Nature. 2017; 550:402–06.
https://doi.org/10.1038/nature24050
PMID:28976970

37. Ivanov A, Pawlikowski J, Manoharan I, van Tuyn J, Nelson DM, Rai TS, Shah PP, Hewitt G, Korolchuk VI, Passos JF, Wu H, Berger SL, Adams PD. Lysosome-mediated processing of chromatin in senescence. J Cell Biol. 2013; 202:129–43.
https://doi.org/10.1083/jcb.201212110
PMID:23816621

38. Glück S, Guey B, Gulen MF, Wolter K, Kang TW, Schmacke NA, Bridgeman A, Rehwinkel J, Zender L, Ablasser A. Innate immune sensing of cytosolic chromatin fragments through cGAS promotes senescence. Nat Cell Biol. 2017; 19:1061–70.
https://doi.org/10.1038/ncb3586
PMID:28759028

39. Yang H, Wang H, Ren J, Chen Q, Chen ZJ. cGAS is essential for cellular senescence. Proc Natl Acad Sci USA. 2017; 114:E4612–20.
https://doi.org/10.1073/pnas.1705499114
PMID:28533362

40. Fane M, Weeraratna AT. How the ageing microenvironment influences tumour progression. Nat Rev Cancer. 2020; 20:89–106.
https://doi.org/10.1038/s41568-019-0222-9
PMID:31836838

41. Da Silva-Álvarez S, Guerra-Varela J, Sobrido-Cameán D, Quelle A, Barreiro-Iglesias A, Sánchez L, Collado M. Cell senescence contributes to tissue regeneration in zebrafish. Aging Cell. 2020; 19:e13052.
https://doi.org/10.1111/acel.13052 PMID:31670873

42. Demaria M, Ohtani N, Youssef SA, Rodier F, Toussaint W, Mitchell JR, Laberge RM, Vijg J, Van Steeg H, Dollé ME, Hoeijmakers JH, de Bruin A, Hara E, Campisi J. An essential role for senescent cells in optimal wound healing through secretion of PDGF-AA. Dev Cell. 2014; 31:722–33.
https://doi.org/10.1016/j.devcel.2014.11.012
PMID:25499914

43. Yun MH, Davaapil H, Brockes JP. Recurrent turnover of senescent cells during regeneration of a complex structure. Elife. 2015; 4:e05505.
https://doi.org/10.7554/eLife.05505
PMID:25942455

44. Muñoz-Espín D, Cañamero M, Maraver A, Gómez-López G, Contreras J, Murillo-Cuesta S, Rodríguez-Baeza A, Varela-Nieto I, Ruberte J, Collado M, Serrano M. Programmed cell senescence during mammalian embryonic development. Cell. 2013; 155:1104–18.
https://doi.org/10.1016/j.cell.2013.10.019
PMID:24238962

45. Storer M, Mas A, Robert-Moreno A, Pecoraro M, Ortells MC, Di Giacomo V, Yosef R, Pilpel N, Krizhanovsky V, Sharpe J, Keyes WM. Senescence is a developmental mechanism that contributes to embryonic growth and patterning. Cell. 2013; 155:1119–30.
https://doi.org/10.1016/j.cell.2013.10.041
PMID:24238961

46. Eggert T, Wolter K, Ji J, Ma C, Yevsa T, Klotz S, Medina-Echeverz J, Longerich T, Forgues M, Reisinger F, Heikenwalder M, Wang XW, Zender L, Greten TF. Distinct functions of senescence-associated immune responses in liver tumor surveillance and tumor progression. Cancer Cell. 2016; 30:533–47.
https://doi.org/10.1016/j.ccell.2016.09.003
PMID:27728804

47. Iannello A, Thompson TW, Ardolino M, Lowe SW, Raulet DH. P53-dependent chemokine production by senescent tumor cells supports NKG2D-dependent tumor elimination by natural killer cells. J Exp Med. 2013; 210:2057–69.
https://doi.org/10.1084/jem.20130783
PMID:24043758

48. Kang TW, Yevsa T, Woller N, Hoenicke L, Wuestefeld T, Dauch D, Hohmeyer A, Gereke M, Rudalska R, Potapova A, Iken M, Vucur M, Weiss S, et al. Senescence surveillance of pre-malignant hepatocytes limits liver cancer development. Nature. 2011; 479:547–51.
https://doi.org/10.1038/nature10599 PMID:22080947

49. Bavik C, Coleman I, Dean JP, Knudsen B, Plymate S, Nelson PS. The gene expression program of prostate fibroblast senescence modulates neoplastic epithelial cell proliferation through paracrine mechanisms. Cancer Res. 2006; 66:794–802.
https://doi.org/10.1158/0008-5472.CAN-05-1716
PMID:16424011

50. Canino C, Mori F, Cambria A, Diamantini A, Germoni S, Alessandrini G, Borsellino G, Galati R, Battistini L, Blandino R, Facciolo F, Citro G, Strano S, et al. SASP mediates chemoresistance and tumor-initiating-activity of mesothelioma cells. Oncogene. 2012; 31:3148–63.
https://doi.org/10.1038/onc.2011.485
PMID:22020330

51. Coppé JP, Kauser K, Campisi J, Beauséjour CM. Secretion of vascular endothelial growth factor by

primary human fibroblasts at senescence. J Biol Chem. 2006; 281:29568–74. https://doi.org/10.1074/jbc.M603307200 PMID:16880208

52. Yang F, Tuxhorn JA, Ressler SJ, McAlhany SJ, Dang TD, Rowley DR. Stromal expression of connective tissue growth factor promotes angiogenesis and prostate cancer tumorigenesis. Cancer Res. 2005; 65:8887–95. https://doi.org/10.1158/0008-5472.CAN-05-1702 PMID:16204060

53. Yoshimoto S, Loo TM, Atarashi K, Kanda H, Sato S, Oyadomari S, Iwakura Y, Oshima K, Morita H, Hattori M, Honda K, Ishikawa Y, Hara E, Ohtani N. Obesity-induced gut microbial metabolite promotes liver cancer through senescence secretome. Nature. 2013; 499:97–101. https://doi.org/10.1038/nature12347 PMID:23803760

54. Basisty N, Kale A, Jeon OH, Kuehnemann C, Payne T, Rao C, Holtz A, Shah S, Sharma V, Ferrucci L, Campisi J, Schilling B. A proteomic atlas of senescence-associated secretomes for aging biomarker development. PLoS Biol. 2020; 18:e3000599. https://doi.org/10.1371/journal.pbio.3000599 PMID:31945054

55. Hernandez-Segura A, de Jong TV, Melov S, Guryev V, Campisi J, Demaria M. Unmasking transcriptional heterogeneity in senescent cells. Curr Biol. 2017; 27:2652–60.e4. https://doi.org/10.1016/j.cub.2017.07.033 PMID:28844647

56. Toso A, Revandkar A, Di Mitri D, Guccini I, Proietti M, Sarti M, Pinton S, Zhang J, Kalathur M, Civenni G, Jarrossay D, Montani E, Marini C, et al. Enhancing chemotherapy efficacy in pten-deficient prostate tumors by activating the senescence-associated antitumor immunity. Cell Rep. 2014; 9:75–89. https://doi.org/10.1016/j.celrep.2014.08.044 PMID:25263564

57. Wang B, Kohli J, Demaria M. Senescent Cells in Cancer Therapy: Friends or Foes? Trends Cancer. 2020; 6:838–57. https://doi.org/10.1016/j.trecan.2020.05.004 PMID:32482536

58. Rao SG, Jackson JG. SASP: tumor suppressor or promoter? yes!. Trends Cancer. 2016; 2:676–87. https://doi.org/10.1016/j.trecan.2016.10.001 PMID:28741506

59. Romagosa C, Simonetti S, López-Vicente L, Mazo A, Lleonart ME, Castellvi J, Ramon y Cajal S. p16(Ink4a) overexpression in cancer: a tumor suppressor gene associated with senescence and high-grade tumors. Oncogene. 2011; 30:2087–97. https://doi.org/10.1038/onc.2010.614 PMID:21297668

60. Coppé JP, Rodier F, Patil CK, Freund A, Desprez PY, Campisi J. Tumor suppressor and aging biomarker p16(INK4a) induces cellular senescence without the associated inflammatory secretory phenotype. J Biol Chem. 2011; 286:36396–403. https://doi.org/10.1074/jbc.M111.257071 PMID:21880712

61. Ortiz-Montero P, Londoño-Vallejo A, Vernot JP. Senescence-associated IL-6 and IL-8 cytokines induce a self- and cross-reinforced senescence/inflammatory milieu strengthening tumorigenic capabilities in the MCF-7 breast cancer cell line. Cell Commun Signal. 2017; 15:17. https://doi.org/10.1186/s12964-017-0172-3 PMID:28472950

62. Zhu J, Woods D, McMahon M, Bishop JM. Senescence of human fibroblasts induced by oncogenic raf. Genes Dev. 1998; 12:2997–3007. https://doi.org/10.1101/gad.12.19.2997 PMID:9765202

63. Di Micco R, Fumagalli M, Cicalese A, Piccinin S, Gasparini P, Luise C, Schurra C, Garre' M, Nuciforo PG, Bensimon A, Maestro R, Pelicci PG, d'Adda di Fagagna F. Oncogene-induced senescence is a DNA damage response triggered by DNA hyper-replication. Nature. 2006; 444:638–42. https://doi.org/10.1038/nature05327 PMID:17136094

64. Ogrunc M, Di Micco R, Liontos M, Bombardelli L, Mione M, Fumagalli M, Gorgoulis VG, d'Adda di Fagagna F. Oncogene-induced reactive oxygen species fuel hyperproliferation and DNA damage response activation. Cell Death Differ. 2014; 21:998–1012. https://doi.org/10.1038/cdd.2014.16 PMID:24583638

65. Aird KM, Zhang G, Li H, Tu Z, Bitler BG, Garipov A, Wu H, Wei Z, Wagner SN, Herlyn M, Zhang R. Suppression of nucleotide metabolism underlies the establishment and maintenance of oncogene-induced senescence. Cell Rep. 2013; 3:1252–65. https://doi.org/10.1016/j.celrep.2013.03.004 PMID:23562156

66. Chakravarti A, Heydon K, Wu CL, Hammond E, Pollack A, Roach M, Wolkov H, Okunieff P, Cox J, Fontanesi J, Abrams R, Pilepich M, Shipley W, and Radiation Therapy Oncology Group. Loss of p16 expression is of prognostic significance in locally advanced prostate cancer: an analysis from the radiation therapy oncology group protocol 86-10. J Clin Oncol. 2003; 21:3328–34. https://doi.org/10.1200/JCO.2003.12.151 PMID:12947069

67. Straume O, Sviland L, Akslen LA. Loss of nuclear p16 protein expression correlates with increased tumor cell proliferation (Ki-67) and poor prognosis in patients with vertical growth phase melanoma. Clin Cancer Res. 2000; 6:1845–53. PMID:10815907

68. Weinberger PM, Yu Z, Haffty BG, Kowalski D, Harigopal M, Sasaki C, Rimm DL, Psyrri A. Prognostic significance of p16 protein levels in oropharyngeal squamous cell cancer. Clin Cancer Res. 2004; 10:5684–91. https://doi.org/10.1158/1078-0432.CCR-04-0448 PMID:15355894

69. Witkiewicz AK, Knudsen KE, Dicker AP, Knudsen ES. The meaning of p16(ink4a) expression in tumors: functional significance, clinical associations and future developments. Cell Cycle. 2011; 10:2497–503. https://doi.org/10.4161/cc.10.15.16776 PMID:21775818

70. Zhao R, Choi BY, Lee MH, Bode AM, Dong Z. Implications of genetic and epigenetic alterations of CDKN2A (p16(INK4a)) in cancer. EBioMedicine. 2016; 8:30–39. https://doi.org/10.1016/j.ebiom.2016.04.017 PMID:27428416

71. Borczuk AC, Taub RN, Hesdorffer M, Hibshoosh H, Chabot JA, Keohan ML, Alsberry R, Alexis D, Powell CA. P16 loss and mitotic activity predict poor survival in patients with peritoneal Malignant mesothelioma. Clin Cancer Res. 2005; 11:3303–08. https://doi.org/10.1158/1078-0432.CCR-04-1884 PMID:15867227

72. Illei PB, Rusch VW, Zakowski MF, Ladanyi M. Homozygous deletion of CDKN2A and codeletion of the methylthioadenosine phosphorylase gene in the majority of pleural mesotheliomas. Clin Cancer Res. 2003; 9:2108–13. PMID:12796375

73. Kamiryo T, Tada K, Shiraishi S, Shinojima N, Nakamura H, Kochi M, Kuratsu J, Saya H, Ushio Y. Analysis of homozygous deletion of the p16 gene and correlation with survival in patients with glioblastoma multiforme. J Neurosurg. 2002; 96:815–22. https://doi.org/10.3171/jns.2002.96.5.0815 PMID:12005388

74. Gan X, Lin X, He R, Lin X, Wang H, Yan L, Zhou H, Qin H, Chen G. Prognostic and clinicopathological significance of downregulated p16 expression in patients with bladder cancer: a systematic review and meta-analysis. Dis Markers. 2016; 2016:5259602. https://doi.org/10.1155/2016/5259602 PMID:27199504

75. Oshima M, Okano K, Muraki S, Haba R, Maeba T, Suzuki Y, Yachida S. Immunohistochemically detected expression of 3 major genes (CDKN2A/p16, TP53, and SMAD4/DPC4) strongly predicts survival in patients with resectable pancreatic cancer. Ann Surg. 2013; 258:336–46. https://doi.org/10.1097/SLA.0b013e3182827a65 PMID:23470568

76. Mihic-Probst D, Mnich CD, Oberholzer PA, Seifert B, Sasse B, Moch H, Dummer R. P16 expression in primary Malignant melanoma is associated with prognosis and lymph node status. Int J Cancer. 2006; 118:2262–68. https://doi.org/10.1002/ijc.21608 PMID:16331607

77. Xing X, Cai W, Shi H, Wang Y, Li M, Jiao J, Chen M. The prognostic value of CDKN2A hypermethylation in colorectal cancer: a meta-analysis. Br J Cancer. 2013; 108:2542–48. https://doi.org/10.1038/bjc.2013.251 PMID:23703248

78. Casella G, Munk R, Kim KM, Piao Y, De S, Abdelmohsen K, Gorospe M. Transcriptome signature of cellular senescence. Nucleic Acids Res. 2019; 47:11476. https://doi.org/10.1093/nar/gkz879 PMID:31612919

79. Liu JY, Souroullas GP, Diekman BO, Krishnamurthy J, Hall BM, Sorrentino JA, Parker JS, Sessions GA, Gudkov AV, Sharpless NE. Cells exhibiting strong *p16^{INK4a}* promoter activation *in vivo* display features of senescence. Proc Natl Acad Sci USA. 2019; 116:2603–11. https://doi.org/10.1073/pnas.1818313116 PMID:30683717

80. Herranz N, Gil J. Mechanisms and functions of cellular senescence. J Clin Invest. 2018; 128:1238–46. https://doi.org/10.1172/JCI95148 PMID:29608137

81. Meyer P, Maity P, Burkovski A, Schwab J, Müssel C, Singh K, Ferreira FF, Krug L, Maier HJ, Wlaschek M, Wirth T, Kestler HA, Scharffetter-Kochanek K. A model of the onset of the senescence associated secretory phenotype after DNA damage induced senescence. PLoS Comput Biol. 2017; 13:e1005741. https://doi.org/10.1371/journal.pcbi.1005741 PMID:29206223

82. Damsky W, Micevic G, Meeth K, Muthusamy V, Curley DP, Santhanakrishnan M, Erdelyi I, Platt JT, Huang L, Theodosakis N, Zaidi MR, Tighe S, Davies MA, et al. mTORC1 activation blocks BrafV600E-induced growth arrest but is insufficient for melanoma formation. Cancer Cell. 2015; 27:41–56. https://doi.org/10.1016/j.ccell.2014.11.014 PMID:25584893

83. Krimpenfort P, Quon KC, Mooi WJ, Loonstra A, Berns A. Loss of p16Ink4a confers susceptibility to metastatic melanoma in mice. Nature. 2001; 413:83–86. https://doi.org/10.1038/35092584 PMID:11544530

84. Shah PP, Donahue G, Otte GL, Capell BC, Nelson DM, Cao K, Aggarwala V, Cruickshanks HA, Rai TS, McBryan T, Gregory BD, Adams PD, Berger SL. Lamin B1 depletion in senescent cells triggers large-scale changes in gene expression and the chromatin landscape. Genes Dev. 2013; 27:1787–99. https://doi.org/10.1101/gad.223834.113 PMID:23934658

85. Hari P, Millar FR, Tarrats N, Birch J, Quintanilla A, Rink CJ, Fernández-Duran I, Muir M, Finch AJ, Brunton VG, Passos JF, Morton JP, Boulter L, Acosta JC. The innate immune sensor toll-like receptor 2 controls the senescence-associated secretory phenotype. Sci Adv. 2019; 5:eaaw0254. https://doi.org/10.1126/sciadv.aaw0254 PMID:31183403

86. Takahashi A, Loo TM, Okada R, Kamachi F, Watanabe Y, Wakita M, Watanabe S, Kawamoto S, Miyata K, Barber GN, Ohtani N, Hara E. Downregulation of cytoplasmic DNases is implicated in cytoplasmic DNA accumulation and SASP in senescent cells. Nat Commun. 2018; 9:1249. https://doi.org/10.1038/s41467-018-03555-8 PMID:29593264

87. Gao M, He Y, Tang H, Chen X, Liu S, Tao Y. cGAS/STING: novel perspectives of the classic pathway. Molecular Biomedicine. 2020; 1:7. https://doi.org/10.1186/s43556-020-00006-z

88. Kim H, Kim H, Feng Y, Li Y, Tamiya H, Tocci S, Ronai ZA. PRMT5 control of cGAS/STING and NLRC5 pathways defines melanoma response to antitumor immunity. Sci Transl Med. 2020; 12:eaaz5683. https://doi.org/10.1126/scitranslmed.aaz5683 PMID:32641491

89. Zhang H, Chen ZH, Savarese TM. Codeletion of the genes for p16INK4, methylthioadenosine phosphorylase, interferon-alpha1, interferon-beta1, and other 9p21 markers in human Malignant cell lines. Cancer Genet Cytogenet. 1996; 86:22–28. https://doi.org/10.1016/0165-4608(95)00157-3 PMID:8616780

90. Huschtscha LI, Moore JD, Noble JR, Campbell HG, Royds JA, Braithwaite AW, Reddel RR. Normal human mammary epithelial cells proliferate rapidly in the presence of elevated levels of the tumor suppressors p53 and p21(WAF1/CIP1). J Cell Sci. 2009; 122:2989–95. https://doi.org/10.1242/jcs.044107 PMID:19638413

91. Kubbutat MH, Jones SN, Vousden KH. Regulation of p53 stability by Mdm2. Nature. 1997; 387:299–303. https://doi.org/10.1038/387299a0 PMID:9153396

92. Wiley CD, Schaum N, Alimirah F, Lopez-Dominguez JA, Orjalo AV, Scott G, Desprez PY, Benz C, Davalos AR, Campisi J. Small-molecule MDM2 antagonists attenuate the senescence-associated secretory phenotype. Sci Rep. 2018; 8:2410. https://doi.org/10.1038/s41598-018-20000-4 PMID:29402901

93. Buj R, Aird KM. P16: cycling off the beaten path. Mol Cell Oncol. 2019; 6:e1677140. https://doi.org/10.1080/23723556.2019.1677140 PMID:31692916

94. Mirzayans R, Andrais B, Hansen G, Murray D. Role of p16(INK4A) in replicative senescence and DNA damage-induced premature senescence in p53-deficient human cells. Biochem Res Int. 2012; 2012:951574. https://doi.org/10.1155/2012/951574 PMID:22924132

95. Birnhuber A, Egemnazarov B, Biasin V, Bonyadi Rad E, Wygrecka M, Olschewski H, Kwapiszewska G, Marsh LM. CDK4/6 inhibition enhances pulmonary inflammatory infiltration in bleomycin-induced lung fibrosis. Respir Res. 2020; 21:167. https://doi.org/10.1186/s12931-020-01433-w PMID:32616042

96. Goel S, DeCristo MJ, Watt AC, BrinJones H, Sceneay J, Li BB, Khan N, Ubellacker JM, Xie S, Metzger-Filho O, Hoog J, Ellis MJ, Ma CX, et al. CDK4/6 inhibition triggers anti-tumour immunity. Nature. 2017; 548:471–75. https://doi.org/10.1038/nature23465 PMID:28813415

97. Guan X, LaPak KM, Hennessey RC, Yu CY, Shakya R, Zhang J, Burd CE. Stromal senescence by prolonged CDK4/6 inhibition potentiates tumor growth. Mol Cancer Res. 2017; 15:237–49. https://doi.org/10.1158/1541-7786.MCR-16-0319 PMID:28039358

98. Yoshida A, Lee EK, Diehl JA. Induction of therapeutic senescence in vemurafenib-resistant melanoma by extended inhibition of CDK4/6. Cancer Res. 2016; 76:2990–3002. https://doi.org/10.1158/0008-5472.CAN-15-2931 PMID:26988987

99. Ruscetti M, Leibold J, Bott MJ, Fennell M, Kulick A, Salgado NR, Chen CC, Ho YJ, Sanchez-Rivera FJ, Feucht J, Baslan T, Tian S, Chen HA, et al. NK cell-mediated cytotoxicity contributes to tumor control by a cytostatic drug combination. Science. 2018; 362:1416–22. https://doi.org/10.1126/science.aas9090 PMID:30573629

100. Hoare M, Ito Y, Kang TW, Weekes MP, Matheson NJ, Patten DA, Shetty S, Parry AJ, Menon S, Salama R, Antrobus R, Tomimatsu K, Howat W, et al. NOTCH1

mediates a switch between two distinct secretomes during senescence. Nat Cell Biol. 2016; 18:979–92. https://doi.org/10.1038/ncb3397 PMID:27525720

101. Faget DV, Ren Q, Stewart SA. Unmasking senescence: context-dependent effects of SASP in cancer. Nat Rev Cancer. 2019; 19:439–53. https://doi.org/10.1038/s41568-019-0156-2 PMID:31235879

102. Fisher DT, Appenheimer MM, Evans SS. The two faces of IL-6 in the tumor microenvironment. Semin Immunol. 2014; 26:38–47. https://doi.org/10.1016/j.smim.2014.01.008 PMID:24602448

103. Ahmed AA, Nordlind K, Hedblad M, Lagerholm B, Schultzberg M, Lidén S. Interleukin (IL)-1 alpha- and -1 beta-, IL-6-, and tumor necrosis factor-alpha-like immunoreactivities in human common and dysplastic nevocellular nevi and Malignant melanoma. Am J Dermatopathol. 1995; 17:222–29. https://doi.org/10.1097/00000372-199506000-00002 PMID:8599429

104. van Tuyn J, Jaber-Hijazi F, MacKenzie D, Cole JJ, Mann E, Pawlikowski JS, Rai TS, Nelson DM, McBryan T, Ivanov A, Blyth K, Wu H, Milling S, Adams PD. Oncogene-expressing senescent melanocytes up-regulate MHC class II, a candidate melanoma suppressor function. J Invest Dermatol. 2017; 137:2197–207. https://doi.org/10.1016/j.jid.2017.05.030 PMID:28647344

105. Balli D, Rech AJ, Stanger BZ, Vonderheide RH. Immune cytolytic activity stratifies molecular subsets of human pancreatic cancer. Clin Cancer Res. 2017; 23:3129–38. https://doi.org/10.1158/1078-0432.CCR-16-2128 PMID:28007776

106. Morrison C, Pabla S, Conroy JM, Nesline MK, Glenn ST, Dressman D, Papanicolau-Sengos A, Burgher B, Andreas J, Giamo V, Qin M, Wang Y, Lenzo FL, et al. Predicting response to checkpoint inhibitors in melanoma beyond PD-L1 and mutational burden. J Immunother Cancer. 2018; 6:32. https://doi.org/10.1186/s40425-018-0344-8 PMID:29743104

107. Wartenberg M, Cibin S, Zlobec I, Vassella E, Eppenberger-Castori S, Terracciano L, Eichmann MD, Worni M, Gloor B, Perren A, Karamitopoulou E. Integrated genomic and immunophenotypic classification of pancreatic cancer reveals three distinct subtypes with prognostic/predictive significance. Clin Cancer Res. 2018; 24:4444–54. https://doi.org/10.1158/1078-0432.CCR-17-3401 PMID:29661773

108. Hoenicke L, Zender L. Immune surveillance of senescent cells—biological significance in cancer- and non-cancer pathologies. Carcinogenesis. 2012; 33:1123–26. https://doi.org/10.1093/carcin/bgs124 PMID:22470164

109. Brenner E, Schörg BF, Ahmetlić F, Wieder T, Hilke FJ, Simon N, Schroeder C, Demidov G, Riedel T, Fehrenbacher B, Schaller M, Forschner A, Eigentler T, et al. Cancer immune control needs senescence induction by interferon-dependent cell cycle regulator pathways in tumours. Nat Commun. 2020; 11:1335. https://doi.org/10.1038/s41467-020-14987-6 PMID:32165639

110. Uphoff CC, Drexler HG. Detection of mycoplasma contaminations. Methods Mol Biol. 2005; 290:13–23. https://doi.org/10.1385/1-59259-838-2:013 PMID:15361652

111. Cerami E, Gao J, Dogrusoz U, Gross BE, Sumer SO, Aksoy BA, Jacobsen A, Byrne CJ, Heuer ML, Larsson E, Antipin Y, Reva B, Goldberg AP, et al. The cBio cancer genomics portal: an open platform for exploring multidimensional cancer genomics data. Cancer Discov. 2012; 2:401–04. https://doi.org/10.1158/2159-8290.CD-12-0095 PMID:22588877

112. Gao J, Aksoy BA, Dogrusoz U, Dresdner G, Gross B, Sumer SO, Sun Y, Jacobsen A, Sinha R, Larsson E, Cerami E, Sander C, Schultz N. Integrative analysis of complex cancer genomics and clinical profiles using the cBioPortal. Sci Signal. 2013; 6:pl1. https://doi.org/10.1126/scisignal.2004088 PMID:23550210

113. Dimri GP, Lee X, Basile G, Acosta M, Scott G, Roskelley C, Medrano EE, Linskens M, Rubelj I, Pereira-Smith O, et al. A biomarker that identifies senescent human cells in culture and in aging skin *in vivo*. Proc Natl Acad Sci U S A. 1995; 92:9363–7. https://doi.org/10.1073/pnas.92.20.9363 PMID:7568133

SUPPLEMENTARY MATERIALS

Supplementary Figures

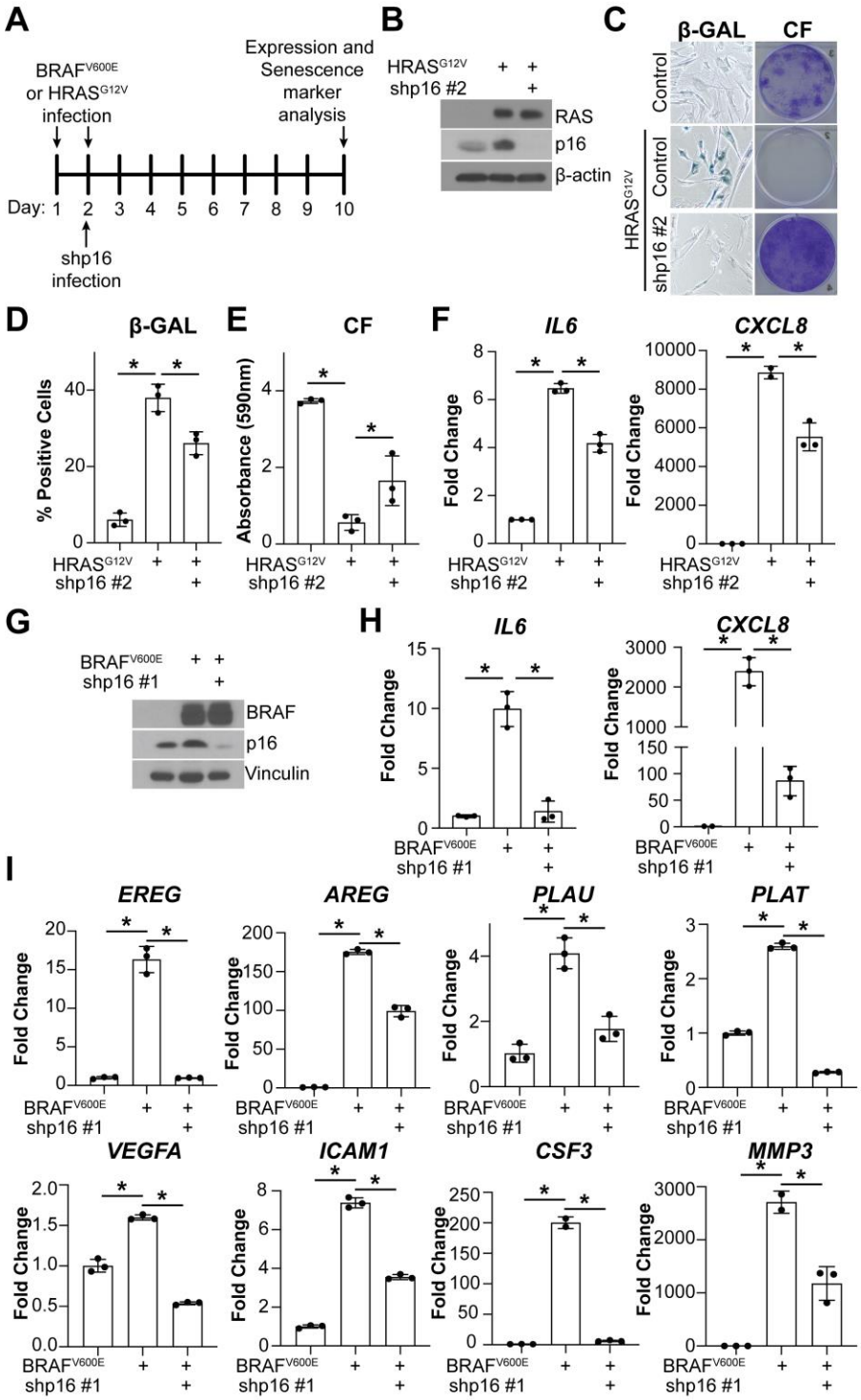

Supplementary Figure 1. Knockdown of p16 using a second hairpin and independent cell line decreases *IL6* and *CXCL8* gene expression in oncogene-induced cells; knockdown of p16 decreases expression of other SASP factors; related to Figure 1. (**A**)

Schematic of the experimental procedure for Figure 1 and Supplementary Figure 1. (**B**–**F**) IMR90s expressing HRAS^{G12V} alone or in combination with a shRNA targeting p16 (shp16 hairpin #2). An empty pBabe retroviral and a shRNA targeting GFP lentiviral vector were used as controls. (**B**) Immunoblot of RAS and p16. β-actin was used as loading control. (**C**) Representative images of senescence-associated β-galactosidase (β-GAL) staining and colony formation (CF). (**D**) Quantification of β-GAL in (**C**). (**E**) Quantification of CF in (**C**). (**F**) *IL6* and *CXCL8* mRNA expression (fold change relative to control mean). (**G**, **H**) Hs 895.Sk cells expressing BRAF^{V600E} alone or in combination with a shRNA targeting p16 (shp16 hairpin #1). An empty pBabe retroviral and a shRNA targeting GFP lentiviral vector were used as controls. (**G**) Immunoblot of BRAF and p16. Vinculin was used as loading control. (**H**) *IL6* and *CXCL8* mRNA expression (fold change relative to control mean). (**I**) IMR90s expressing BRAF^{V600E} alone or in combination with a shRNA targeting p16 (shp16 hairpin #1). An empty pBabe retroviral and a shRNA targeting GFP lentiviral vector were used as controls. mRNA expression of the indicated genes (fold change relative to control mean). For all RT-qPCR, expression of target genes was normalized against multiple reference genes. Data normalized against *MRPL9* are shown. n=3/group and mean±SD. 1 out of 3 experiments is shown. *p<0.05.

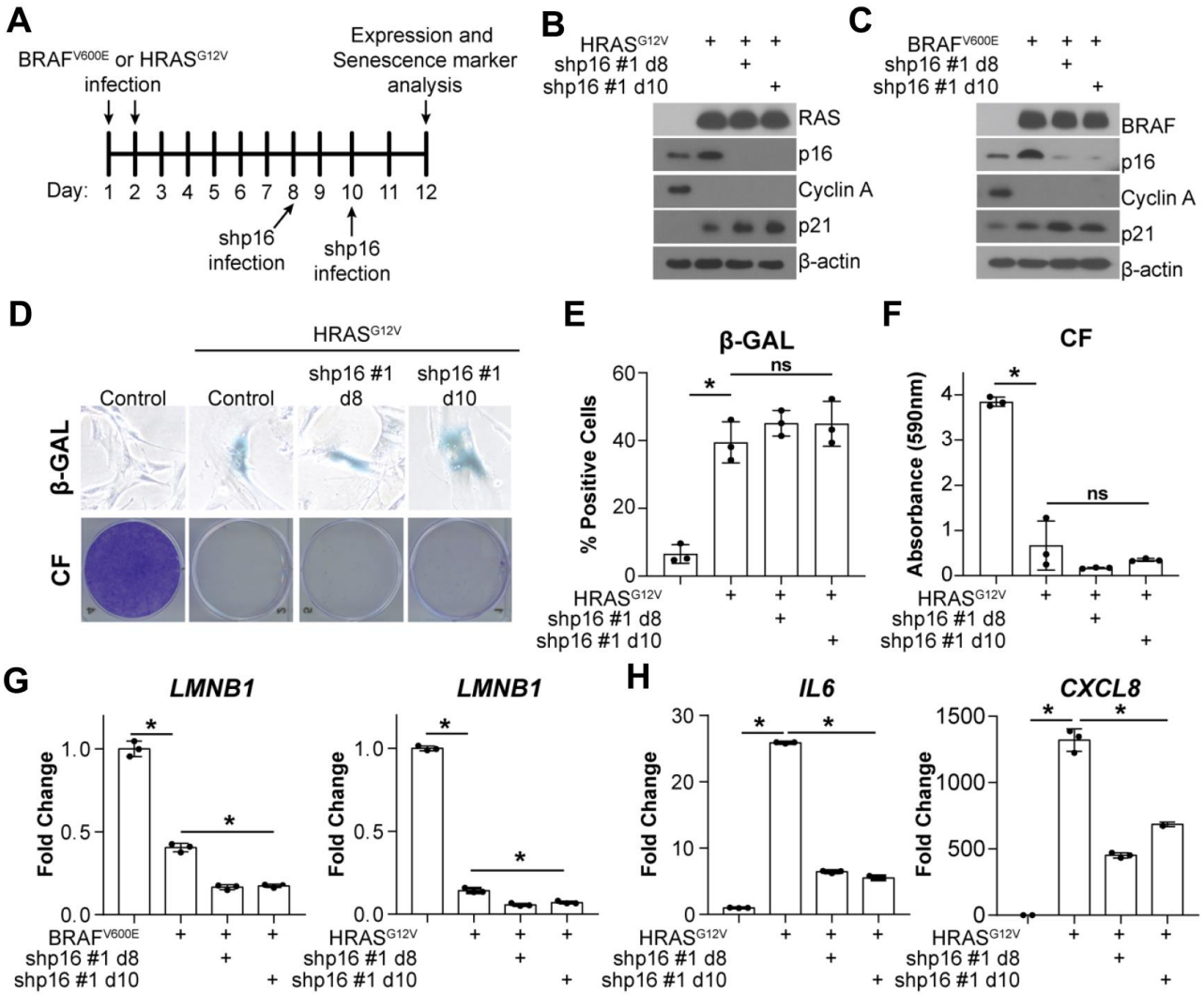

Supplementary Figure 2. Knockdown of p16 at later timepoints decreases *IL6* and *CXCL8* but does affect other senescence markers including *LMNB1*; related to Figure 2. (**A**) Schematic of experimental procedure for Figure 2 and Supplementary Figure 2. (**B**–**H**) IMR90s expressing either BRAF^{V600E} or HRAS^{G12V} alone or in combination with a shRNA targeting p16 (shp16 hairpin #1). An empty pBabe retroviral and a shRNA targeting GFP lentiviral vector were used as controls. (**B**, **C**) Immunoblot of the indicated proteins. β-actin was used as loading control. (**D**) Representative images of senescence-associated β-galactosidase (β-GAL) staining and colony formation (CF). (**E**) Quantification of β-GAL in (**D**). (**F**) Quantification of CF in (**D**). (**G**) *LMNB1* mRNA expression (fold change relative to control mean). (**H**) *IL6* and *CXCL8* mRNA expression (fold change relative to control mean). For all RT-qPCR, expression of target genes was normalized against multiple reference genes. Data normalized against *MRPL9* are shown. n=3/group and mean±SD. 1 out of 3 experiments is shown. *p<0.05, ns = not significant.

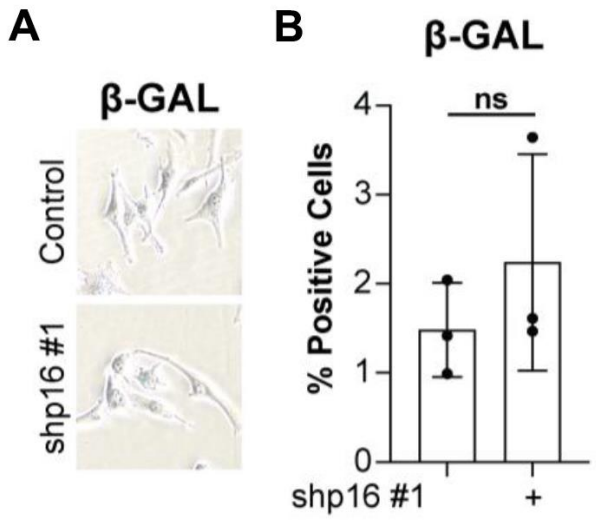

Supplementary Figure 3. Melanoma cells with stable knockdown of p16 do not have less spontaneous senescent cells in culture; related to Figure 3. (**A**, **B**) SKMel28 melanoma cells with stable knockdown of p16 (shp16 hairpin #1). An shRNA targeting GFP lentiviral vector was used as control. (**A**) Representative images of senescence-associated β-galactosidase (β-GAL) staining. (**B**) Quantification of β-GAL in (**A**). ns = not significant.

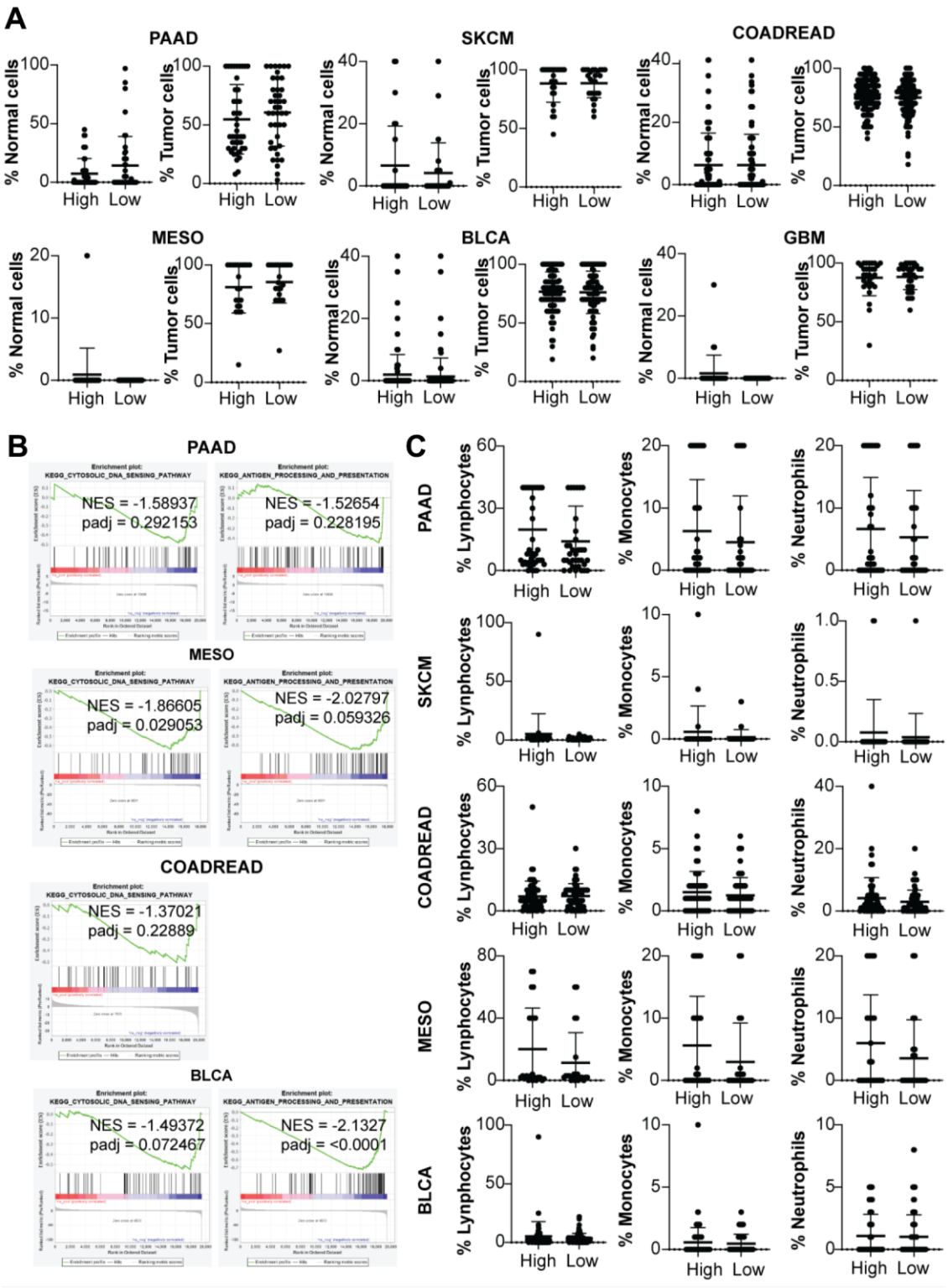

Supplementary Figure 4. Tumors with low CDKN2A expression show decreased inflammation-related signatures not associated with changes in percentage of normal cells or immune cell infiltration; related to Figure 4. (**A**) Percentage of normal and tumor cells seen on an OCT-embedded tissue slide reported by TCGA between CDKN2A-high (i.e., p16-high) and CDKN2A-low (i.e., p16-low) in the indicated tumors. (**B**) Inflammation related negatively enriched terms in p16-low vs. p16-high expressing tumors. (**C**) Percentage of lymphocytes, monocytes, and neutrophils seen on an OCT-embedded tissue slide reported by TCGA between p16-high and p16-low in the indicated tumors. SKCM (skin cutaneous melanoma), PAAD (pancreatic adenocarcinoma), COADREAD (colorectal adenocarcinoma), MESO (mesothelioma), BLCA (bladder urothelial carcinoma), GBM (glioblastoma multiforme), NES (negative enrichment score).

Supplementary Tables

Please browse Full Text version to see the data of Supplementary Tables 1–4.

Supplementary Table 1. 232 total unique SASP genes including soluble factors and exosomes obtained from [54].

Supplementary Table 2. Differential expression analysis of *CDKN2A*-low (p16-low) vs. *CDKN2A*-high (p16-high) tumors obtained from TCGA.

Supplementary Table 3. Gene set enrichment analysis for *CDKN2A*-low (p16-low) vs. *CDKN2A*-high (p16-high) tumors using Casella et al. senescence expression signature.

Supplementary Table 4. Primer sequences.